

文章编号:1000-0550(2025)04-1178-21

鄂尔多斯盆地西缘乌拉力克组笔石带划分及对沉积演化的指示

高小洋¹,王传尚²,何文祥¹,张建伍³,封莉⁴,严婧文¹,万涛⁵,朱建斌⁶,徐鹏程³,
王斌⁷,胡勇¹

1.长江大学资源与环境学院,武汉 430100
2.中国地质调查局武汉地质调查中心古生物与地质环境演化湖北省重点实验室,武汉 430100
3.中国石油长庆油田分公司勘探开发研究院,西安 710000
4.中国石油长庆油田分公司勘探事业部,西安 710018
5.中国石化中原油田物探研究院,河南濮阳 457000
6.中国石油长庆油田分公司第一采油厂,陕西延安 716000
7.中国石油长庆油田分公司长庆实业集团有限公司,西安 710018

摘要 【目的】鄂尔多斯盆地西缘乌拉力克组发育一套海相笔石页岩,近些年在该套笔石页岩中不断发现有天然气显示,并可产生工业油流,表明乌拉力克组存在较大勘探潜力。探讨乌拉力克组的笔石发育特征,建立笔石生物地层格架,分析该组的沉积演化规律,为下一步油气勘探开发奠定基础。【方法】通过分析取心井的笔石特征,明确乌拉力克组的时代归属,开展单井笔石带划分并建立生物地层格架,结合岩性发育规律分析黑色页岩的空间演化,并依据笔石体的演化对海侵的响应探讨相对海平面的变化规律。【结果】(1)乌拉力克组隶属奥陶世中晚期达瑞威尔阶—桑比阶,并依据笔石发育特征将乌拉力克组分为四个笔石带,从下到上依次发育 *Pterograptus elegans* 带、*Jiangxigraptus vagus* 带、*Nemagraptus gracilis* 带、*Climacograptus bicornis* 带;(2)通过对比回分析笔石带发育特征,认为研究区乌拉力克组北部 QT9 井附近发育完整的四个笔石带,南部缺失 *Pterograptus elegans* 与 *Jiangxigraptus vagus* 带;(3)乌拉力克组的 *Pterograptus elegans* 与 *Nemagraptus gracilis* 带为两个海侵期,向上至 *Climacograptus bicornis* 带相对海平面逐渐降低。【结论】乌拉力克组底部的黑色页岩由 QT9 井的 *Pterograptus elegans* 带到 YinT2 井的 *Nemagraptus gracilis* 带表现出强烈的穿时性,沿鄂尔多斯地块西缘向南地层逐渐变年轻,指示沉积中心逐渐向南迁移。

关键词 笔石带划分;生物地层格架;乌拉力克组;沉积演化

第一作者简介 高小洋,男,1995年出生,博士,储层地质学,E-mail: 884570830@qq.com

通信作者 胡勇,男,博士,副教授,E-mail: 64421847@qq.com

中图分类号 P534.42 Q915.2 文献标志码 A

DOI: 10.14027/j.issn.1000-0550.2024.077

CSTR: 32268.14/j.cjxb.62-1038.2024.077

0 引言

中奥陶世乌拉力克组笔石泥页岩层是近年来鄂尔多斯盆地西缘海相页岩气勘探的主要目的层。长庆油田在鄂尔多斯盆地西缘奥陶系中不断发现天然气显示,忠4井在乌拉力克组试气获得 $4 \times 10^4 \text{ m}^3/\text{d}$ 的工业气流,证明盆地西缘乌拉力克组发育有效海相烃源岩^[1-2],但目前对其地层及沉积环境演化特征认

识不足,制约着勘探进展。

笔石是一类生活在古代海洋中的动物,其命名最早由瑞典分类学家林奈于 1735 年创立的类化石属“Graptolithus”演变而来^[3]。笔石种类多、分布广、演化快、特征明显,被誉为奥陶纪、志留纪和泥盆纪早期地层研究的标准化石。笔石动物每隔几十万年就会产生新物种,且笔石的分布规律与沉积环境息息

收稿日期:2024-04-07;修回日期:2024-06-11;录用日期:2024-07-22;网络出版日期:2024-07-22

基金项目:国家自然科学基金项目(52174019);湖北省教育厅科学研究计划资助项目(D20201302)[Foundation: National Natural Science Foundation of China, No. 52174019; Educational Commission of Hubei Province of China, No. D20201302]

相关^[4-5]。前人通过分析笔石化石发育特征及组合样式,在不同地区笔石特征建立了多种笔石带划分方案,进而分析地层的发育特征,明确沉积演化规律。张娣等^[5]通过分析扬子西南缘五峰组—龙马溪组露头和钻井取心的笔石特征,建立等时地层格架,探讨笔石带的分布与沉积环境,明确优质页岩的发育特征及演化规律;梁峰等^[6]通过分析川南地区五峰组—龙马溪组页岩笔石特征,建立了8个笔石带,认为黑色页岩的沉积时间与沉积速率在不同区块存在显著差异,黑色页岩沉积中心不断向北迁移;白灵麒等^[7]通过鉴定内蒙古苏尼特左旗北部巴彦呼舒组的笔石化石,认为该组地层时代为中—晚奥陶世,发育于近源大陆斜坡沉积环境。

自20世纪80年代以来,前人对于鄂尔多斯盆地西缘乌拉力克组的笔石带及时代归属问题开展了较多研究,但仍存在较大争议。例如:傅力浦等^[8]、马占荣等^[9]通过对比岩性及上下地层笔石特征,将鄂尔多斯桌子山地区的乌拉力克组划为 *Glyptograptus teretiusculus* 与 *Nemagraptus gracilis* 2个笔石带;张文华等^[10]认为乌拉力克组最多包含 *Nemagraptus gracilis* 带底部;孙肇才等^[11]将乌拉力克组限定在

Glyptograptus teretiusculus 带,将该组对应于达瑞威尔阶最上部。由于前人研究仅局限在剖面露头,缺乏钻井取心资料,致使对鄂尔多斯盆地西缘乌拉力克组的笔石特征认识不足,导致地层划分及其发育模式尚不明确。另外,前人认为乌拉力克组为镶边台地沉积模式^[12-13],但未对其演化过程进行研究。

本文通过对鄂尔多斯盆地西缘乌拉力克组6口取心井的笔石进行鉴定,明确乌拉力克组时代归属,进一步划分研究区的笔石带,分析地层发育特征,建立生物地层格架,并在此基础上结合岩性特征讨论乌拉力克组的沉积演化规律,旨在为下一步油气勘探开发奠定基础。

1 区域地质概况

鄂尔多斯盆地西缘处于鄂尔多斯盆地东、西部构造交汇区,整体呈南北向展布(图1a),在早古生代,盆地西缘位于鄂尔多斯地块与古秦岭洋之间,具被动大陆边缘性质^[14-15]。受加里东运动与全球海平面变化的影响,在中晚奥陶世,其东部与华北地台接壤,西部延伸至贺兰海槽,也是祁连海所影响到的最东部^[9]。在中奥陶世克里摩里期,海侵范围达到最

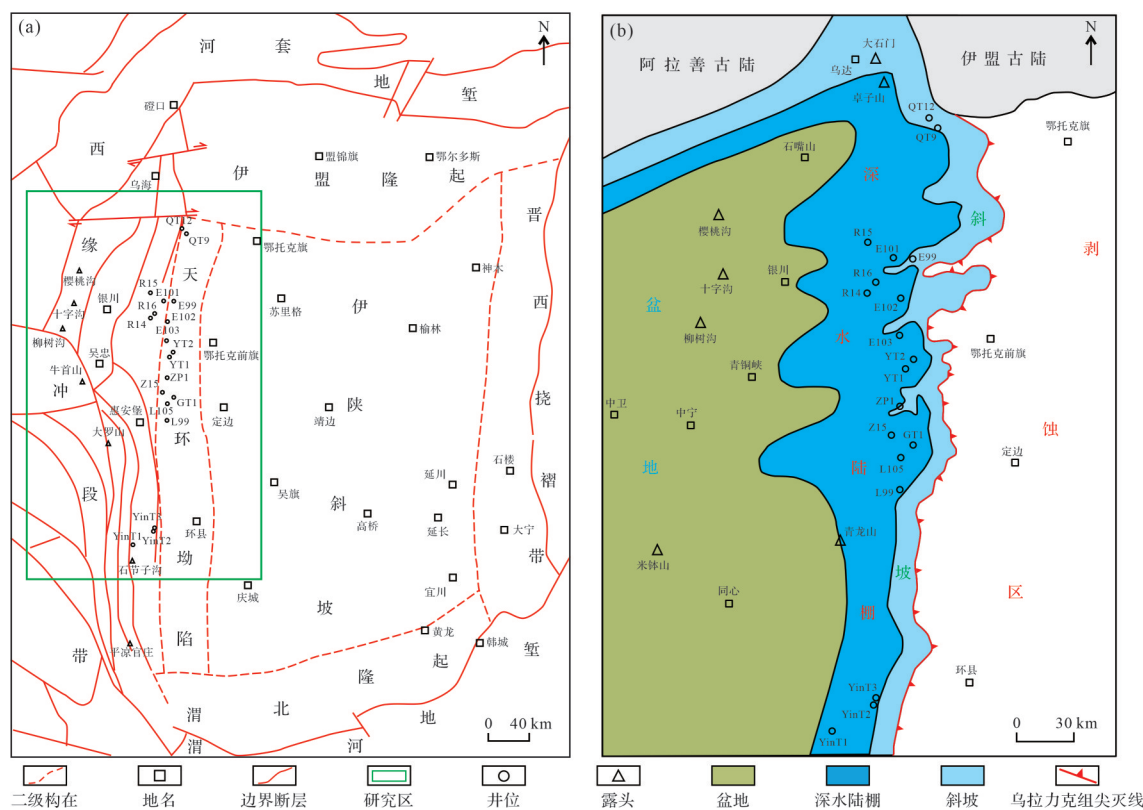


图1 (a)工区位置;(b)古地理展布图(据文献[12]修改)

Fig.1 (a) Location of study area; (b) paleogeographic distribution map (modified from reference [12])

大^[16],至乌拉力克组沉积时期,西缘地区继续裂陷,东部继续抬升,由东向西依次发育浅水灰质斜坡、深水陆棚和海槽等相带^[12](图1b)。晚奥陶世,海水向西南方向海退,致使西缘地区海相沉积结束^[17]。

研究区奥陶系中—上统依次发育三道坎组、桌子山组、克里摩里组、乌拉力克组与拉什仲组^[9](图2),奥陶系与上覆、下伏地层均呈不整合接触^[15,18],其中乌拉力克组发育大量的笔石化石,为笔石地层划分的研究奠定了较好的基础。本文通过笔石鉴定,在前人研究的基础上^[19-20]进一步理清了乌拉力克组的笔石带特征及层位归属,认为乌拉力克组属于中晚奥陶世达瑞威尔阶—桑比阶(图2),其自下而上发育 *Pterograptus elegans* 带(精美翼笔石带)、*Jiangxigraptus vagus* 带(蜿蜒江西笔石带)、*Nemagraptus gracilis* 带(纤细丝笔石带)、*Climacograptus bicornis* 带(双刺栅笔石带)。

2 工区内主要笔石特征及笔石带划分

乌拉力克组系指克里摩里组石灰岩之上的一

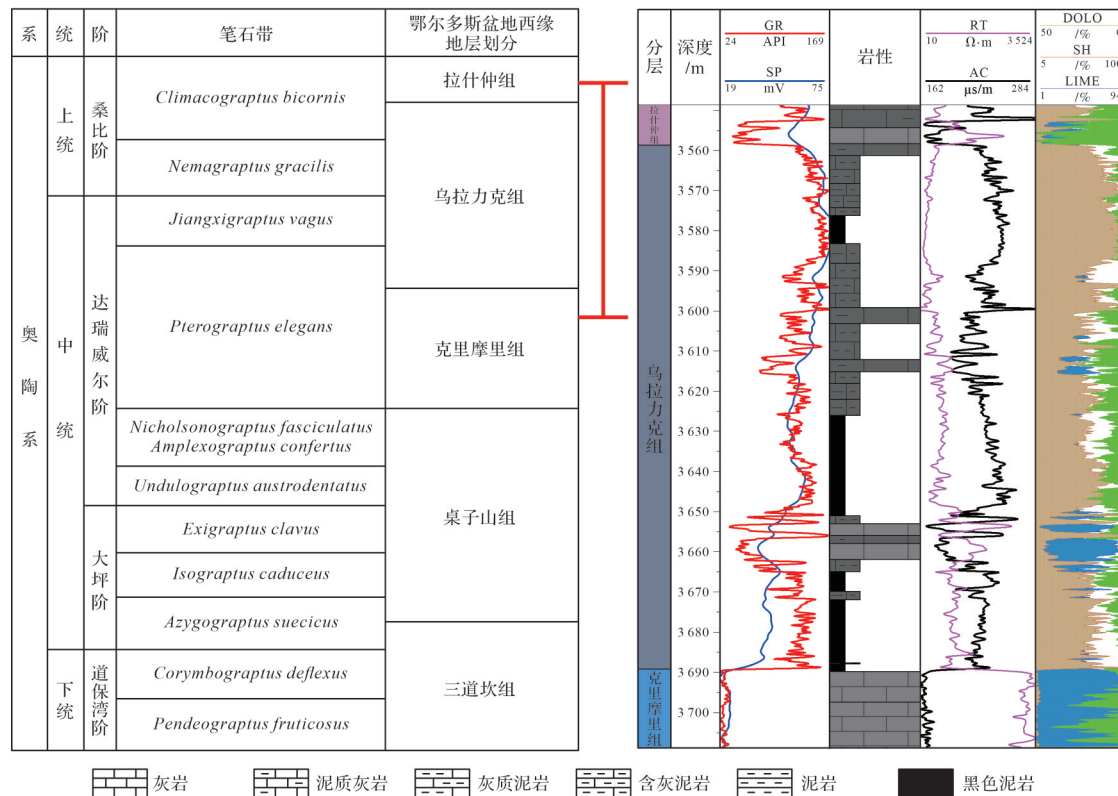


图2 研究区地层划分与笔石带发育特征

桌子山组与三道坎组对应的笔石带是前人依据牙形刺的对比得出(据文献[9])

Fig.2 Stratigraphic division and development of the graptolite zones in the study area

The graptolite zones in the Zhuozishan and Sandaokan Formations were determined based on conodont identification in previous studies (after reference [9])

套以深灰色、灰黑色含笔石泥页岩,中夹数层灰色—深灰色泥质灰岩、灰岩的地层,其顶部泥页岩与拉什仲组底部石灰岩为界。目前对该套层系地层发育及演化模式没有清晰的认识,制约着页岩气勘探开发的进程。本文通过分析钻井岩心的笔石发育特征,建立笔石生物地层格架,分析地层及沉积演化规律。

2.1 乌拉力克组时代分析

通过对研究区E102井、E103井、L105井、QT9井、R16井、YinT2井、QT12井的取心段进行连续取样,根据笔石分枝情况、笔石枝生长方向、笔石始端与胞管的发育情况对研究区笔石的种属进行鉴定,明确笔石化石的垂向发育特征。研究区共识别出桑比阶两个笔石带和达瑞威尔阶上部的两个笔石带,共计笔石28属47种(表1)。

工区内常见笔石化石(图3)包括中晚奥陶世笔石 *Climacograptus bicornis* (图3a)、*Cryptograptus marcidus* (图3b)、*Crypto-graptus tricornis* (图3g)等。虽然也见有早奥陶世 *Kalpinograptus* 笔石属化石(图3c),但此属化石分布时间较长;见有晚奥陶世桑比期

表1 研究区各笔石带所含笔石种属及主要发育的钻井

Table 1 Graptolite species contained in each graptolite zone and main drilling wells for development in the study area

笔石带	属种	笔石带中所含化石包括	主要钻井
Climacograptus bicornis带	17属23种	<i>Dicellograptus angulatus</i> , <i>Dicellograptus pumilus</i> , <i>Dicellograptus sp.</i> , <i>Unicornigraptus xinjiangensis</i> , <i>Didymograptus sp.</i> , <i>Archiclimacograptus arctus</i> , <i>Archiclimacograptus meridionalis</i> , <i>Archiclimacograptus modestus</i> , <i>Archiclimacograptus sp.</i> , <i>Haddingograptus eurystoma</i> , <i>Haddingograptus flexibilis</i> , <i>Haddingograptus oliveri</i> , <i>Haddingograptus sp.</i> , <i>Hustedograptus teretiusculus</i> , <i>Pseudazygograptus incurvus</i> , <i>Pseudoclimacograptus scharenbergi</i> , <i>Pseudoclimacograptus sp.</i> , <i>Acrograptus sp.</i> , <i>Jiangxigraptus salopiensis</i> , <i>Jiangxigraptus sextans</i> , <i>Jiangxigraptus sp.</i> , <i>Syndyograptus sinensis</i> , <i>Ningxiagraptus yangtzensis</i> , <i>Dicranograptus sinensis</i> , <i>Amplexograptus sp.</i> , <i>Pronormalograptus regularis</i> , <i>Pronormalograptus sp.</i> , <i>Climacograptus bicornis</i> , <i>Climacograptus sp.</i> , <i>Orthograptus apiculatus</i> , <i>Orthograptus paracalcaratus</i> , <i>Orthograptus sp.</i> , <i>Orthograptus whitfieldi</i>	Z15、YinT2、L105
Nemagraptus gracilis带	12属12种	<i>Dicellograptus pumilus</i> , <i>Dicellograptus sp.</i> , <i>Dicellograptus angulatus</i> , <i>Dicellograptus geniculatus</i> , <i>Acanthograptus sp.</i> , <i>Didymograptus sp.</i> , <i>Archiclimacograptus caelatus</i> , <i>Archiclimacograptus sp.</i> , <i>Archiclimacograptus angulatus</i> , <i>Archiclimacograptus meridionalis</i> , <i>Archiclimacograptus riddellensis</i> , <i>Archiclimacograptus arctus</i> , <i>Reteograptus geinitzianus</i> , <i>Haddingograptus oliveri</i> , <i>Haddingograptus sp.</i> , <i>Haddingograptus eurystoma</i> , <i>Haddingograptus flexibilis</i> , <i>Hallograptus sp.</i> , <i>Hustedograptus teretiusculus</i> , <i>Pseudazygograptus incurvus</i> , <i>Pseudoclimacograptus sp.</i> , <i>Pseudoclimacograptus acies</i> , <i>Pseudoclimacograptus scharenbergi</i> , <i>Acrograptus sp.</i> , <i>Jiangxigraptus divaricatus</i> , <i>Jiangxigraptus sp.</i> , <i>Jiangxigraptus gurleyi</i> , <i>Jiangxigraptus mui</i> , <i>Jiangxigraptus salopiensis</i> , <i>Jiangxigraptus exilis</i> , <i>Jiangxigraptus sextans</i> , <i>Kalpinograptus sp.</i> , <i>Glossograptus fimbriatus</i> , <i>Glossograptus hincksi</i> , <i>Dicranograptus brevicaulis</i> , <i>Dicranograptus ramosus angustus</i> , <i>Dicranograptus sinensis</i> , <i>Nemagraptus gracilis</i> , <i>Amplexograptus sp.</i> , <i>Cryptograptus marcoides</i> , <i>Cryptograptus tricornis</i> , <i>Proclimacograptus angustatus</i> , <i>Pronormalograptus euglyphus</i> , <i>Pronormalograptus sp.</i> , <i>Pronormalograptus acicularis</i> , <i>Climacograptus sp.</i> , <i>Orthograptus whitfieldi</i> , <i>Orthograptus apiculatus</i> , <i>Orthograptus paracalcaratus</i>	L105、YinT2、R16、QT9、E102、E103
Jiangxigraptus vagus带	21属38种	<i>Dicellograptus geniculatus</i> , <i>Didymograptus sp.</i> , <i>Archiclimacograptus sp.</i> , <i>Reteograptus geinitzianus</i> , <i>Haddingograptus sp.</i> , <i>Hustedograptus teretiusculus</i> , <i>Pseudazygograptus incurvus</i> , <i>Pseudoclimacograptus scharenbergi</i> , <i>Acrograptus sp.</i> , <i>Jiangxigraptus mui</i> , <i>Jiangxigraptus vagus</i> , <i>Jiangxigraptus cf. vagus</i> , <i>Jiangxigraptus sextans</i> , <i>Abrograptus formosus</i> , <i>Glossograptus fimbriatus</i> , <i>Dicranograptus sinensis</i> , <i>Cryptograptus tricornis</i> , <i>Orthograptus apiculatus</i> , <i>Orthograptus sp.</i> , <i>Pseudoclimacograptus scharenbergi</i> , <i>Haddingograptus sp.</i> , <i>Hustedograptus sp.</i> , <i>Didymograptus sp.</i> , <i>Pterograptus elegans</i> , <i>Kalpinograptus sp.</i> , <i>Amplexograptus sp.</i> , <i>pseudazygograptus incurvus</i> , <i>Hustedograptus teretiusculus</i> , <i>Cryptograptus tricornis</i> , <i>Archiclimacograptus modestus</i> , <i>Dicellograptus sp.</i> , <i>Haddingograptus oliveri</i> , <i>Archiclimacograptus angulatus</i> , <i>Reteograptus geinitzianus</i> , <i>Jiangxigraptus gurleyi</i> , <i>Archiclimacograptus sp.</i> , <i>Cryptograptus marcoides</i> , <i>Haddingograptus eurystoma</i> , <i>Apoglossograptus uniformis</i> , <i>Jiangxigraptus salopiensis</i> , <i>Dicellograptus geniculatus</i> , <i>Jiangxigraptus sp.</i> , <i>Jiangxigraptus mui</i> , <i>Glossograptus fimbriatus</i> , <i>Archiclimacograptus meridionalis</i> , <i>Acrograptus sp.</i> , <i>Pronormalograptus acicularis</i> , <i>Orthograptus apiculatus</i>	R16、QT9、QT9

早期的带化石 *Nemagraptus gracilis* (图 3d) 以及达瑞威尔阶晚期化石 *Jiangxigraptus vagus* (图 3e) 与 *Pterograptus elegans* (图 3f)。综合笔石分布延限^[21](图 4) 分析认为, 乌拉力克组应为中奥陶世中晚期达瑞威尔阶—桑比阶。

2.2 各笔石带笔石发育特征

2.2.1 *Pterograptus elegans* 带

该带以带化石 *Pterograptus elegans* 的首次出现为底界标志^[20,22], 该种在乌拉力克组乌海大石门剖面克里摩里组上段、新疆阿克苏四石场剖面萨尔干组首次出现^[23-24]。该种广泛分布于华南和塔里木的斜坡

相地层中^[20], 还常见于北欧、美国、阿根廷等国, 在全球广泛分布^[25]。本次研究中 *Pterograptus elegans* 带主要发育 *Pterograptus elegans* (图 5a), *Archiclimacograptus modestus* (图 5b), *Pseudoclimacograptus scharenbergi* (图 5c), *Hustedograptus teretiusculus* (图 5d), *Kalpinograptus sp.* (图 5e), *Cryptograptus tricornis* (图 5f), *Jiangxigraptus salopiensis* (图 5g), *Dicellograptus geniculatus* (图 5h), *Acrograptus sp.* (图 5i) 等笔石属种(其余的笔石属种见表 1, 共识别出 18 属 23 种)。研究区 *Pterograptus elegans* 带的笔石化石主要分布在 QT9 井附近(图 5)。

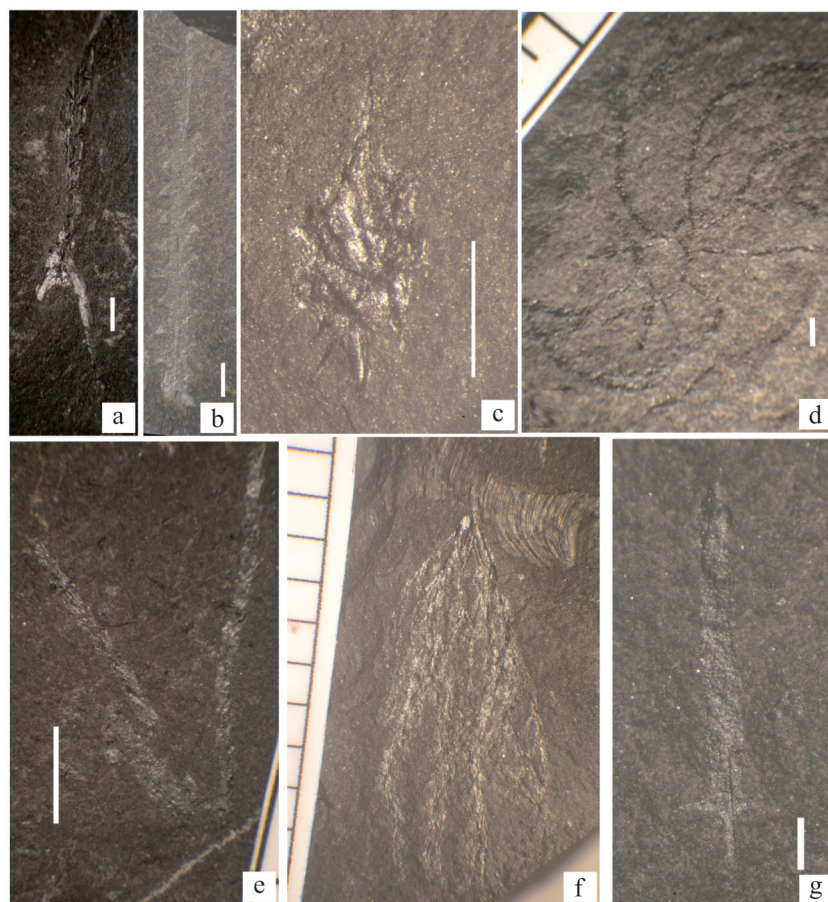


图3 乌拉力克组主要笔石特征

(a) *Climacograptus bicornis*, L105井, 4 256.28 m; (b) *Cryptograptus marcidus*, R16井, 2 880.06 m; (c) *Kalpinograptus* sp., QT9井, 4 742.14 m; (d) *Nemagraptus gracilis*, R16井, 2 880.06 m; (e) *Jiangxigraptus vagus*, R16井, 2 881.93 m; (f) *Pterograptus elegans*, QT9井, 4 746.06 m; (g) *Cryptograptus tricornis*, E102井, 3 947.33 m

Fig.3 Main graptolites in the Wulalik Formation

(a) *Climacograptus bicornis*, well L105, 4 256.28 m; (b) *Cryptograptus marcidus*, well R16, 2 880.06 m; (c) *Kalpinograptus* sp., well QT9, 4 742.14 m; (d) *Nemagraptus gracilis*, well R16, 2 880.06 m; (e) *Jiangxigraptus vagus*, well R16, 2 881.93 m; (f) *Pterograptus elegans*, well QT9, 4 746.06 m; (g) *Cryptograptus tricornis*, well E102, 3 947.33 m

2.2.2 *Jiangxigraptus vagus* 带

该带以叉笔石 *Jiangxigraptus vagus* 的首现为底界标志, 该种在全球分布范围广, 前人在全球多个剖面笔石鉴定中发现, *Jiangxigraptus vagus* 的首次出现往往位于 *Nemagraptus gracilis* 带之下, 且其地层延限较短, 前人在多个地区建立了 *Jiangxigraptus vagus* 带^[26-27]。Chen et al.^[28] 也在中国西北地区建立了 *Jiangxi-graptusvagus* 带, 以取代传统的 *H.teretiusculus* 带, 为本次研究奠定了基础。本次研究中 *Jiangxigraptus vagus* 带(图6)主要发育 *Jiangxigraptus sextans* (图6a), *Jiang-xigraptus vagus* (图6b, d~e), *Abrograptus Formosus*(图6c)等笔石属种, 共识别出21属38种(表1)。研究区 *Jiangxigraptus vagus* 带化石主要分布在R16井、QT9井。

2.2.3 *Nemagraptus gracilis* 带

该带以笔石化石 *Nemagraptus gracilis* 的首现为标志, 是晚奥陶世桑比阶下部带化石, 也是桑比阶底界的标志性化石^[29-30]。在我国华北地块西缘^[31]、华南^[32]和塔里木^[33]等地均有发现。本次研究中 *Nemagraptus gracilis* 带主要发育 *Archiclimacograptus caelatus* (图7a), *Haddingograptus flexibilis* (图7b), *Pseudoclimacograptus scharenbergi*(图7c), *Pseudazygograptus incurvus*(图7d), *Acrograptus* sp.(图7e), *Jiangxigraptus di-varicatus*(图7f), *Kalpinograptus* sp.(图7g), *Glossograptus fimbriatus*(图7h), *Dicranograptus ramosus angustus*(图7i), *Nemagraptus gracilis*(图7j), *Cryptograptus marcidus*(图7k), *Orthograptus whitfieldi*(图7l)等笔石属种, 共识别出12属12种(表1)。该化石在工区内

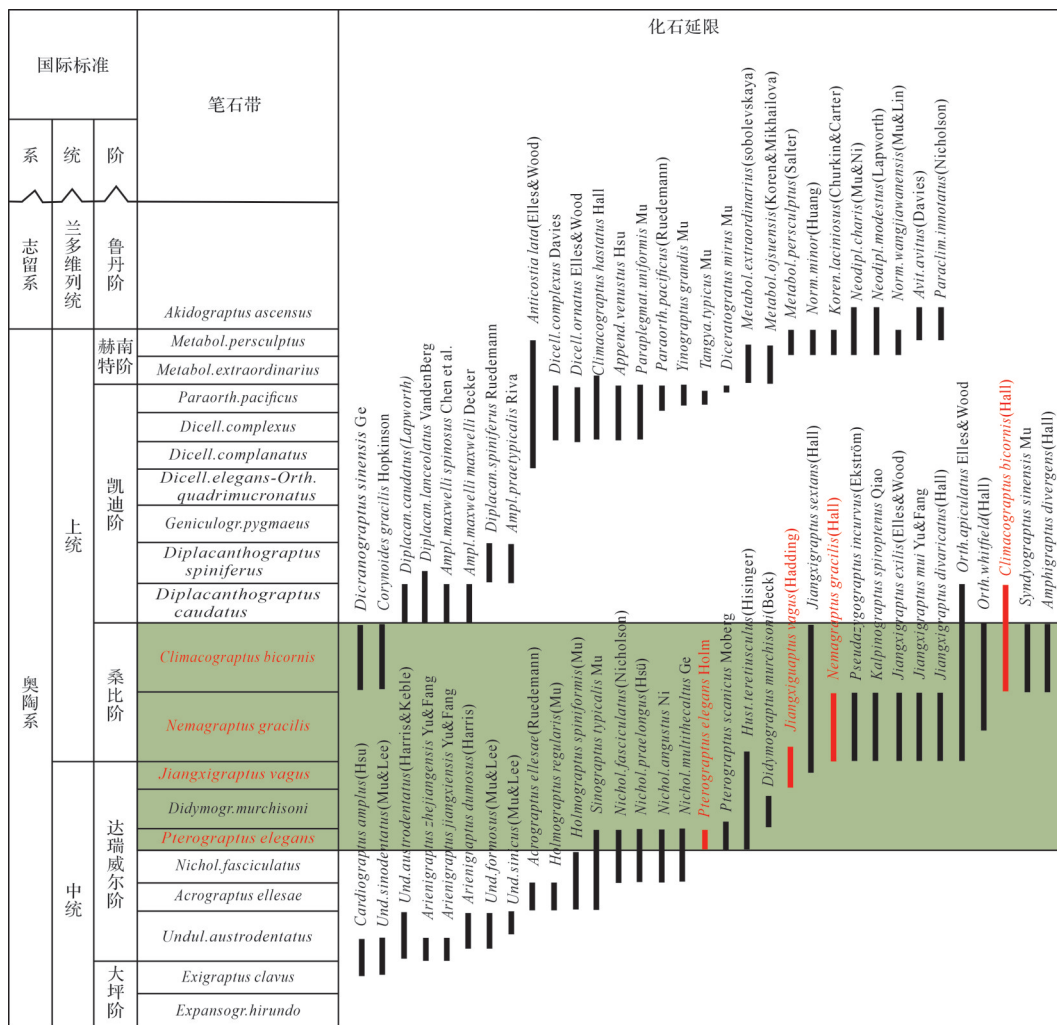


图4 奥陶系中一上统笔石延限图(据文献[21]修改)

Fig.4 Range of graptolites in the Middle to Upper Ordovician (modified from reference [21])

分布范围广,包括有L105井、YinT2井、R16井、QT9井、E102井、E103井。

2.2.4 *Climacograptus bicornis* 带

该带以*Climacograptus bicornis*的首现作为底界标志^[28]。该类笔石还分布在华北地块西缘的甘肃平凉^[31]、陕西陇县^[34]、塔里木柯坪^[21]、华南扬子区(庙坡组)^[35]和江南斜坡带(胡乐组)^[36]等地区。本次研究中*Climacograptus bicornis*带(图8)主要发育*Climacograptus bicornis*(图8a, e~f),*Pseudoclimacograptus scharenbergi*(图8b),*Orthograptus apiculatus*(图8c)等笔石属种,共识别出17属23种(表1)。在研究区内主要存在于Z15井、YinT2井、L105井(图8)。

3 笔石带划分及分布特征分析

古生物化石是地层划分的重要依据。其中笔石

动物群随着时间的推移会迅速变化,在奥陶纪时期,笔石动物的种数与数量达到顶峰,生存环境也得到极大的扩展^[4]。由于受沉积环境影响较大,笔石可作为生物地层解释和岩石序列定年的主要对象^[37-38]。乌拉力克组发育大量笔石化石,通过分析取心井的笔石生物带特征,进一步明确乌拉力克组的地层发育模式。受取心段影响,本文对L105井、YinT2井、R16井、QT9井、E102井、E103井的笔石带进行划分,建立研究区的生物地层格架。其中R16井、E102井、E103井乌拉力克组顶部缺乏取心段,通过分析地层发育及演化特征认为其顶部可能存在*Climacograptus bicornis*带。

3.1 单井笔石带划分

3.1.1 L105井

L105井位于宁夏回族自治区吴忠市盐池县冯记

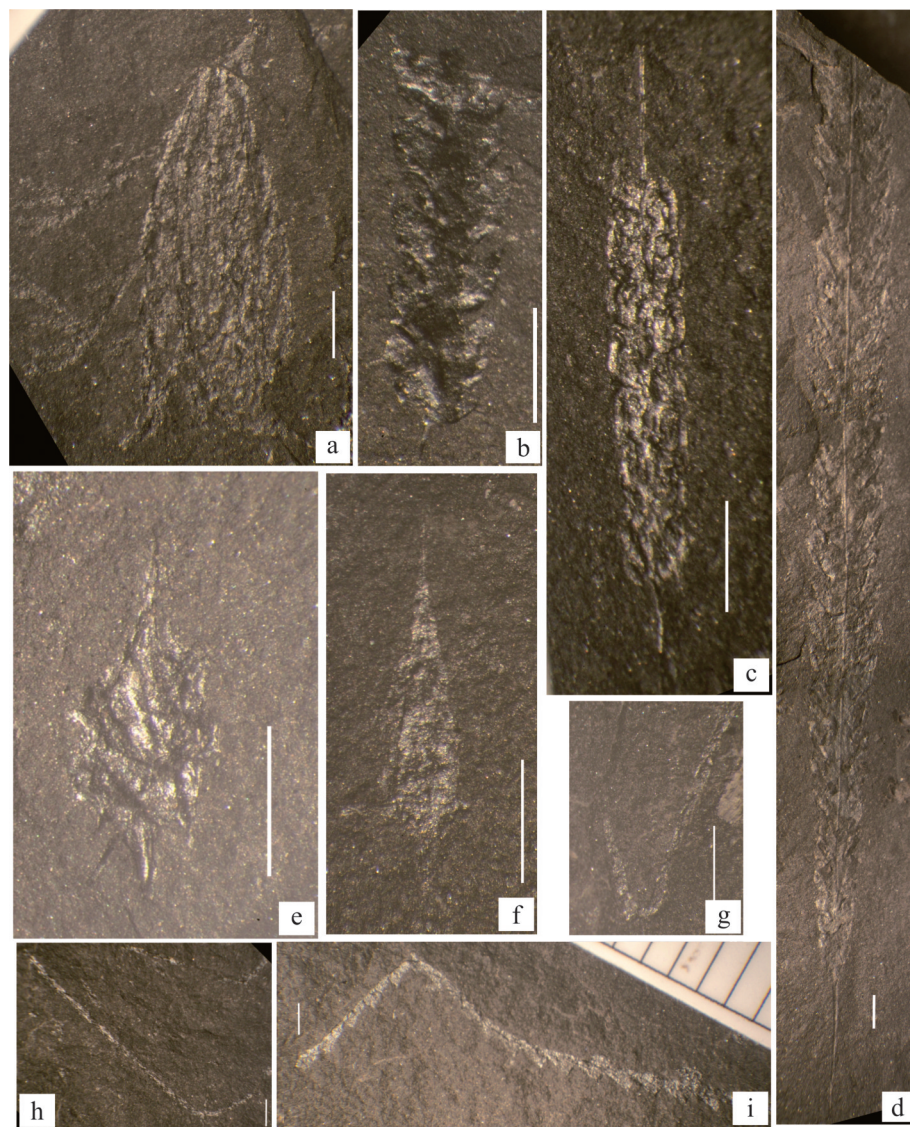


图5 *Pterograptus elegans* 带主要笔石化石特征(QT9井,白线比例尺为1 mm)

(a) *Pterograptus elegans*, 4 742.14 m; (b) *Archiclimacograptus modestus*, 4 742.14 m; (c) *Pseudoclimacograptus scharenbergi*, 4 742.60 m; (d) *Hustedograptus teretiusculus*, 4 753.55 m; (e) *Kalpinograptus* sp., 4 742.14 m; (f) *Cryptograptus tricornis*, 4 742.60 m; (g) *Jiangxigraptus salopiensis*, 4 748.53 m; (h) *Dicellograptus geniculatus*, 4 750.37 m; (i) *Acograptus* sp., 4 755.95 m

Fig.5 Main graptolite fossil features of the *Pterograptus elegans* zone (well QT9, white line = 1 mm)

(a) *Pterograptus elegans*, 4 742.14 m; (b) *Archiclimacograptus modestus*, 4 742.14 m; (c) *Pseudoclimacograptus scharenbergi*, 4 742.60 m; (d) *Hustedograptus teretiusculus*, 4 753.55 m.; (e) *Kalpinograptus* sp., 4 742.14 m; (f) *Cryptograptus tricornis*, 4 742.60 m; (g) *Jiangxigraptus salopiensis*, 4 748.53 m; (h) *Dicellograptus geniculatus*, 4 750.37 m; (i) *Acograptus* sp., 4 755.95 m

沟乡暴记春村,依据岩性特征认为乌拉力克组深度介于4 242.00 m~4 301.00 m,厚度为59.00 m,取心井段为4 217.80~4 229.50 m与4 250.00~4 293.60 m,该井在4 262.60 m出现*Nemagraptus gracilis*,其上约5.19 m出现*Cilmacograptus bicornis*,因此将*Nemagraptus gracilis*带和*Cilmacograptus bicornis*带的界线置于后者在本井首现的位置4 257.41 m。从笔石群面貌看,本井下部笔石化石均为*Nemagraptus gracilis*带,上部笔石化石均为*Cilmacograptus bicornis*带。其

中取心段4 217.80~4 229.50 m为拉什仲组,其笔石特征属于*Climacograptus bicornis*带(图9)。

3.1.2 YinT2井

银探2井地理位置隶属于甘肃省环县车道乡刘渠村,构造位置属于鄂尔多斯盆地西缘冲断带,乌拉力克组深度介于3 838.30~3 934.90 m,厚度为96.60 m,笔石鉴定段为3 860.00~3 884.90 m与3 922.60~3 929.60 m(图10)。根据笔石化石面貌,该井乌拉力克的取心段组发育*Climacograptus bicornis*带下部和

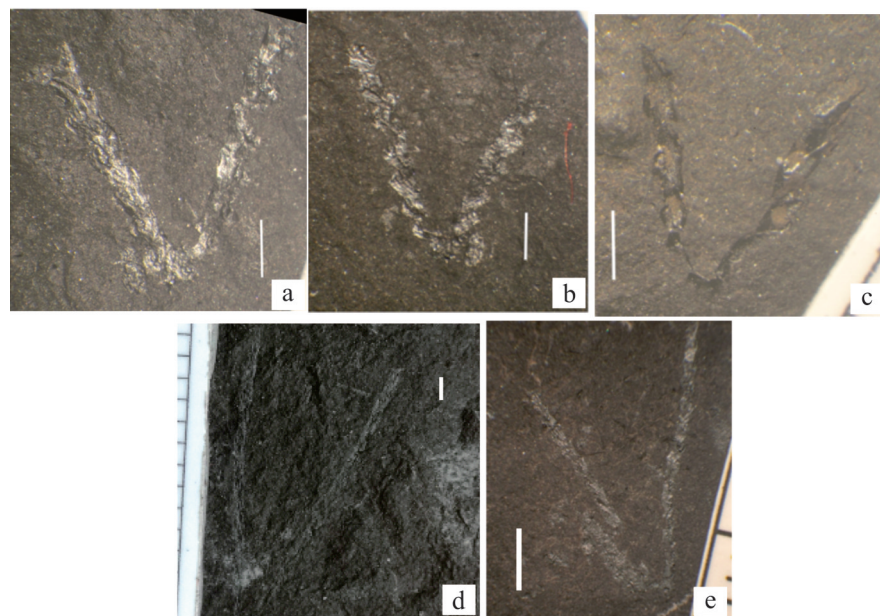


图 6 *Jiangxigraptus vagus* 带主要笔石化石特征(白线比例尺为 1 mm)

(a) *Jiangxigraptus sextans*, QT9井, 4 739.25 m; (b) *Jiangxigraptus vagus*, QT9井, 4 739.25 m; (c) *Abrograptus Formosus*, QT9井, 4 738.81 m; (d) *Jiangxigraptus vagus*, ZP1井, 井深4 274.00 m; (e) *Jiangxigraptus vagus*, R16井, 2 881.93 m

Fig.6 Characteristic graptolite fossils of the *Jiangxigraptus vagus* zone (white line = 1 mm)

(a) *Jiangxigraptus sextans*, well QT9, 4 739.25 m; (b) *Jiangxigraptus vagus*, well QT9, 4 739.25 m; (c) *Abrograptus Formosus*, well QT9, 4 738.81 m; (d) *Jiangxigraptus vagus*, well ZP1, 4 274.00 m; (e) *Jiangxigraptus vagus*, well R16, 2 881.93 m

Nemagraptus gracilis 带上部,两带界线应在 3 866.82 m 和 3 871.50 m 之间,现将界线置于 *Climaocograptus bicornis* 最初出现的 3 866.82 m 处。

3.1.3 R16 井

R16 井位于内蒙古自治区鄂尔多斯鄂托克前旗芒哈图乡哈沙图嘎查,构造上属于鄂尔多斯盆地西缘冲断带,乌拉力克组深度介于 2 763.00~2 897.60 m,厚度 134.60 m,笔石鉴定取样段为 2 790.00~2 800.60 m 和 2 857.00~2 885.60 m(图 11)。识别出 *Jiangxigraptus vagus* 和 *Nemagraptus gracilis* 两个笔石带,尽管在 2 880.06 m 发现 *Nemagraptus gracilis*,但其下 2 881.93 m 所采集的笔石化石,仍呈现 *Nemagraptus gracilis* 带的笔石面貌,因此将该带底界的界线置于 2 881.93 m。2 884.17 m 处见 *Nemagraptus gracilis* 带下伏笔石带的带化石 *Jiangxigraptus vagus*,尽管该化石可上延至 *Nemagraptus gracilis* 带,而在 2 882.93 m 已见到该化石,同时,此处尚无其他化石,确认为 *Jiangxigraptus vagus* 带,故将 2 884.17 m 及以下地层置于 *Jiangxigraptus vagus* 带。

3.1.4 QT9 井

QT9 井隶属于内蒙古自治区鄂尔多斯鄂托克旗阿尔巴斯苏木赛乌苏嘎查,构造位置属于鄂尔多斯

盆地天环坳陷。其乌拉力克组深度介于 4 622.50~4 670.80 m,厚度 98.30 m,取样段深度介于 4 738.00~4 758.80 m。本次研究共识别出 *Jiangxigraptus vagus* 与 *Pterograptus elegans* 等两个笔石带。鉴于在 4 742.14 m 发现 *Pterograptus elegans*,其上 4 741.42 m 发现 *Jiangxigraptus vagus*,可大致确定两个笔石带,即下部的 *Pterograptus elegans* 带与上部的 *Jiangxigraptus vagus* 带,后者只采集了下部的笔石化石,该部分可与 Chen et al.^[28] 的 *Didymograptus murchisoni* 带对比。上述两个笔石带的界线暂置于 *Jiangxigraptus vagus* 的首现位置,即 4 741.42 m 处(图 12)。

由于邻井 QT12 在 5 038.40 m 识别出 *Nemagraptus gracilis* 带的带化石,证明在该处上下发育 *Nemagraptus gracilis* 带,并且该处发育大套泥灰岩与灰岩,与 QT9 井 4 693.00~4 728.00 m 的灰岩与泥灰岩可对比,故 QT9 井乌拉力克组也可能发育 *Nemagraptus gracilis* 带,参考测井曲线变化特征暂将 QT9 井 *Nemagraptus gracilis* 带与 *Jiangxigraptus vagus* 带界限置于 4 718.60 m(图 13)。前人通过对比牙形刺与笔石化石特征认为,克里摩里组发育 *Pterograptus elegans* 带^[9],故 QT9 井乌拉力克组的 *Pterograptus elegans* 带可下延至克里摩里组(图 12)。

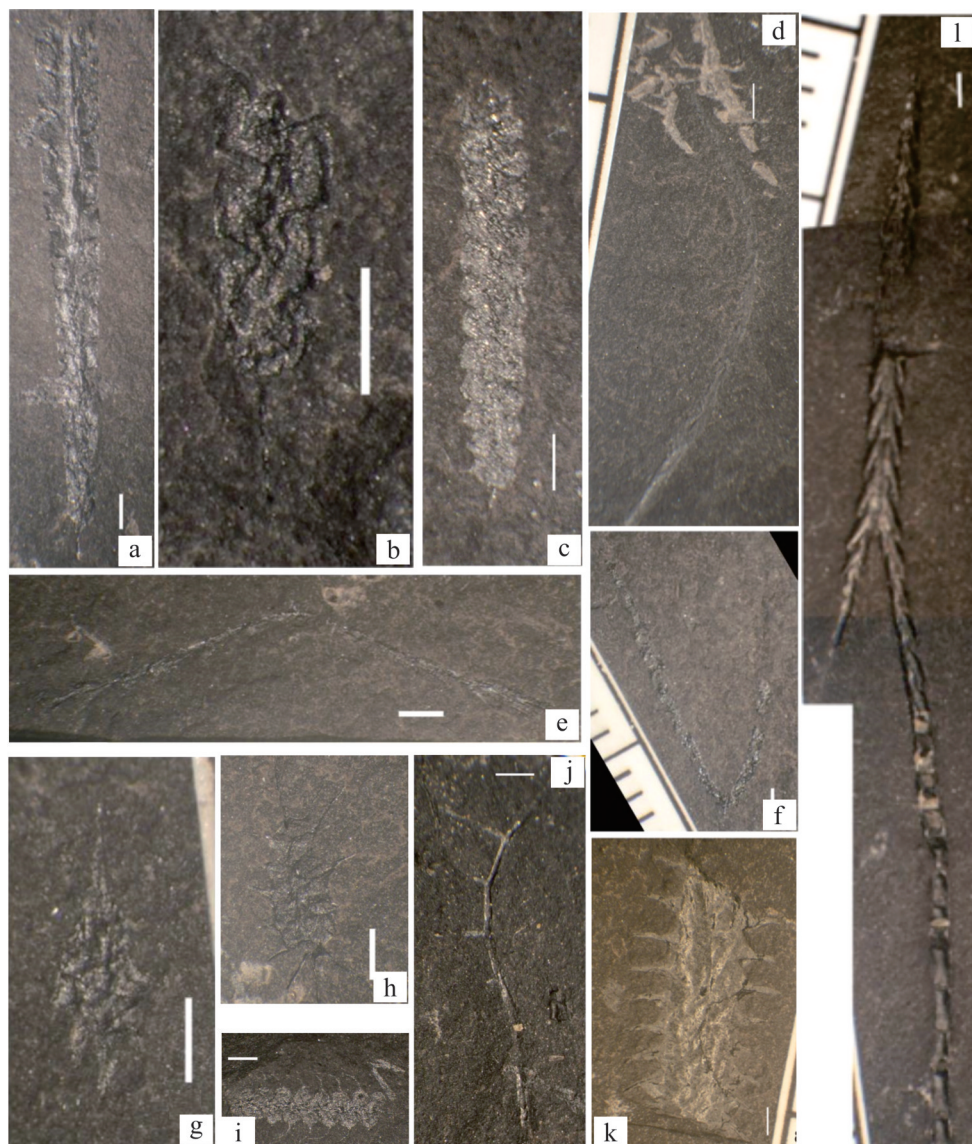


图 7 *Nemagraptus gracilis* 带主要笔石化石特征(白线比例尺为 1 mm)

(a) *Archiclimacograptus caelatus*, E103 井, 3 944.92 m; (b) *Haddingograptus flexibilis*, E102 井, 3 676.13 m; (c) *Pseudoclimacograptus scharenbergi*, E103 井, 3 946.81 m; (d) *Pseudazygograptus incurvus*, R16 井, 2 868.47 m; (e) *Acrograptus* sp., E102 井, 3 679.33 m; (f) *Jiangxigraptus divaricatus*, E102 井, 3 632.49 m; (g) *Kalpinograptus* sp., E103 井, 3 944.92 m; (h) *Glossograptus fimbriatus*, R16 井, 2 867.84 m; (i) *Dicranograptus ramosus angustus*, L105 井, 4 280.30 m; (j) *Nemagraptus gracilis*, L105 井, 4 262.60 m; (k) *Cryptograptus marcidus*, R16 井, 2 880.06 m; (l) *Orthograptus whitfieldi*, E102 井, 3 947.33 m

Fig.7 Main graptolite fossil characteristics of the *Nemagraptus gracilis* zone (white line = 1 mm)

(a) *Archiclimacograptus caelatus*, well E103, 3 944.92 m; (b) *Haddingograptus flexibilis*, well E102, 3 676.13 m; (c) *Pseudoclimacograptus scharenbergi*, well E103, 3 946.81 m; (d) *Pseudazygograptus incurvus*, well R16, 2 868.47 m; (e) *Acrograptus* sp., well E102, 3 679.33 m; (f) *Jiangxigraptus divaricatus*, well E102, 3 632.49 m; (g) *Kalpinograptus* sp., well E103, 3 944.92 m; (h) *Glossograptus fimbriatus*, well R16, 2 867.84 m; (i) *Dicranograptus ramosus angustus*, well L105, 4 280.30 m; (j) *Nemagraptus gracilis*, well L105, 4 262.60 m; (k) *Cryptograptus marcidus*, well R16, 2 880.06 m; (l) *Orthograptus whitfieldi*, well E102, 3 947.33 m

3.1.5 E102 井

E102 井隶属于内蒙古自治区鄂尔多斯鄂托克前旗布拉格苏木哈沙图嘎查, 构造位置属于鄂尔多斯盆地天环坳陷, 乌拉力克组深度介于 3 559.40~3 691.70 m, 样品取样段深度介于 3 630.00~3 636.00 m 和 3 676.00~3 698.60 m。由于该井笔石化石保存较差, 且未发现带化石, 但笔石化石的面貌总体呈现

Nemagraptus gracilis 带的特点, 鉴于 *Glossograptus hincksii* 在下部 3 685.21 m 出现, 该种是 *Nemagraptus gracilis* 带下伏笔石带的典型分子, 但前人在 *Nemagraptus gracilis* 带中也有发现^[23], 故 *Nemagraptus gracilis* 带与下伏笔石带的界线不明确。与 *Nemagraptus gracilis* 带共生的笔石分子 *Jiangxigraptus sextans*、*Cryptograptus tricornis*、*Pseudazygograptus incurvus* 出现于 4 677.30 m

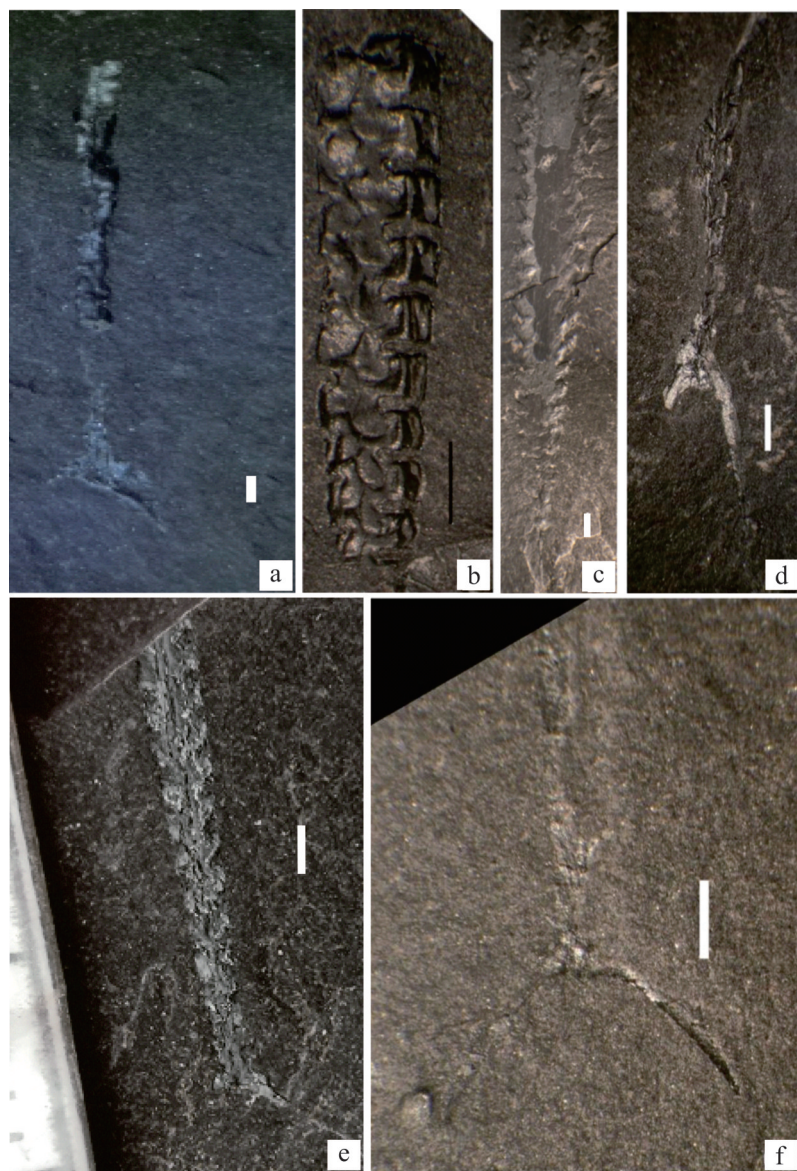


图8 *Climacograptus bicornis* 带主要笔石化石特征(白线比例尺为1 mm)

(a) *Climacograptus bicornis*, Z15井, 4 210.24 m; (b) *Pseudoclimacograptus scharenbergi*, L105井, 4 250.74 m; (c) *Orthograptus apiculatus*, L105井, 4 255.67 m; (d) *Climacograptus bicornis*, L105井, 4 256.28 m; (e) *Climacograptus bicornis*, YinT2井, 3 862.61 m; (f) *Climacograptus bicornis*, L105井, 4 257.41 m

Fig.8 Main graptolite fossil characteristics of the *Climacograptus bicornis* zone (white line = 1 mm)

(a) *Climacograptus bicornis*, well Z15, 4 210.24 m; (b) *Pseudoclimacograptus scharenbergi*, well L105, 4 250.74 m; (c) *Orthograptus apiculatus*, well L105, 4 255.67 m; (d) *Climacograptus bicornis*, well L105, 4 256.28 m; (e) *Climacograptus bicornis*, well YinT2, 3 862.61 m; (f) *Climacograptus bicornis*, well L105, 4 257.41 m

处,距乌拉力克组底界约11.00 m,暂将*Nemagraptus gracilis*带底界放至乌拉力克组与克里摩里组界线处(图14)。

3.1.6 E103井

E103井位于内蒙古自治区鄂托克前旗上海庙镇特布德嘎查,构造位置位于鄂尔多斯盆地天环坳陷,其乌拉力克组深度介于3 889.50~3 950.00 m,

取样段为3 943.40~3 960.20 m。该井笔石化石保存较差,根据笔石化石的总体面貌,尽管未发现*Nemagraptus gracilis*,但与其共生的笔石,特别是*Pseudazygograptus incurvus*、*Cryptograptus tricornis*、*Orthograptus apiculatus*、*Jiangxigraptus sextans*、*Reteograptus geinitzianus*等笔石化石的发现,表明该段黑色页岩应属*Nemagraptus gracilis*带,但顶底界限不明确。

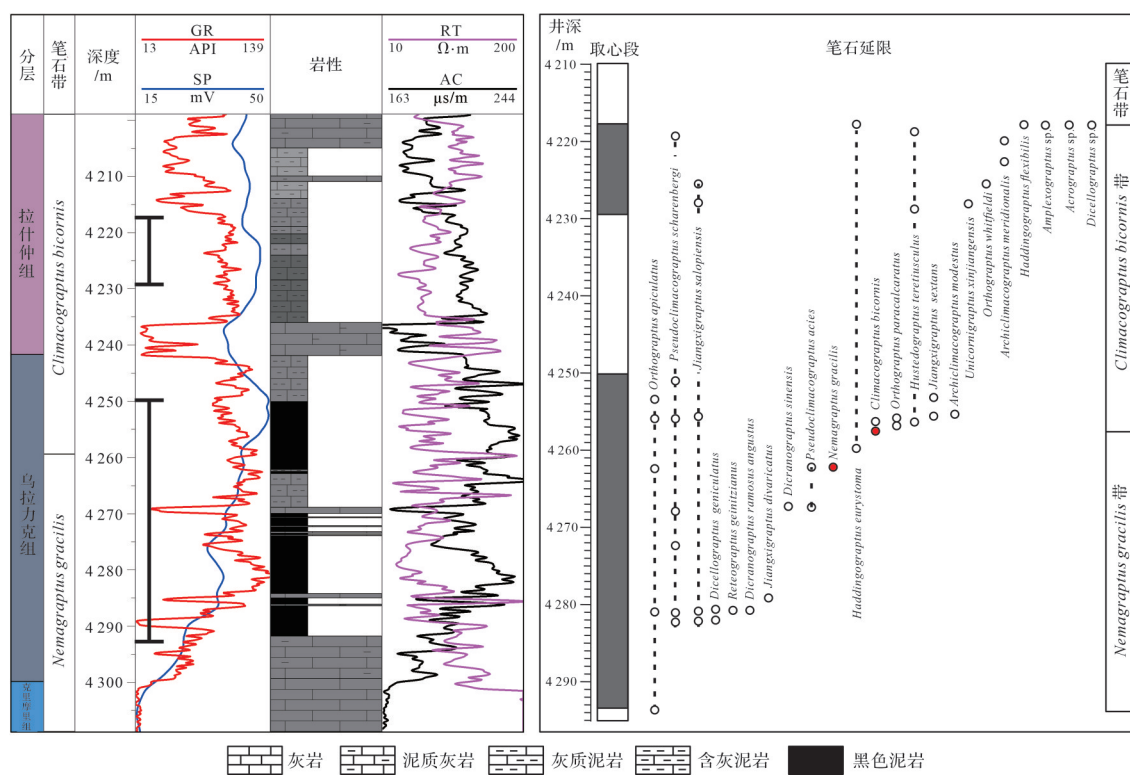


图9 L105井乌拉力克组笔石延限图

Fig.9 Graptolite range chart for the Wulalike Formation at well L105

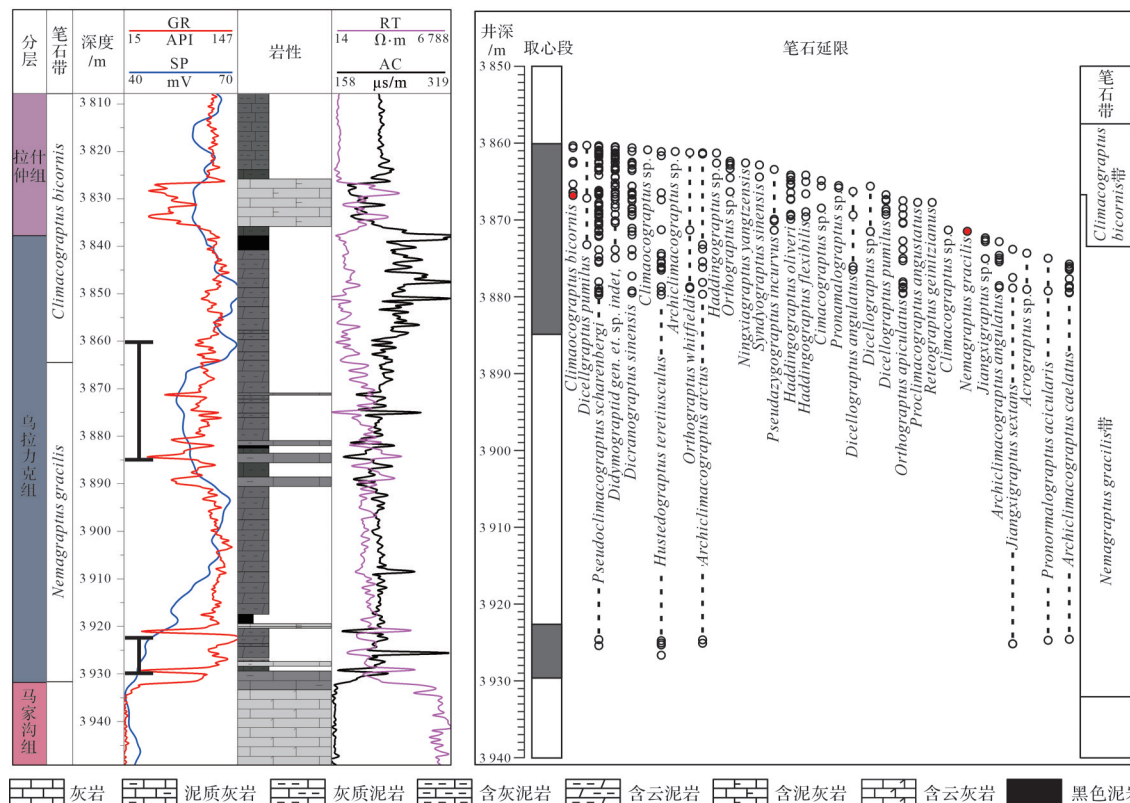


图10 YinT2井乌拉力克组笔石延限图

Fig.10 Graptolite range chart for the Wulalike Formation at well YinT2

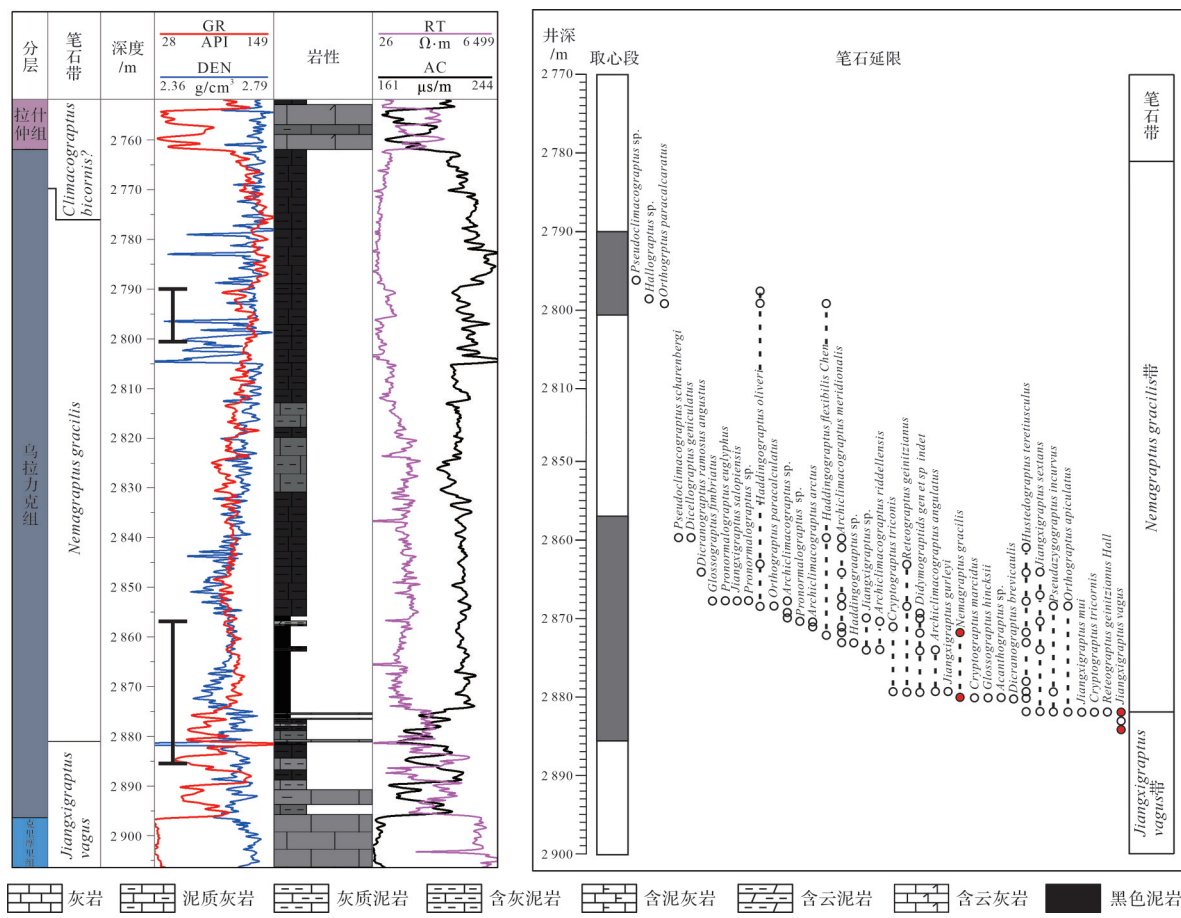


图 11 R16 井乌拉力克组笔石延限图

Fig.11 Graptolite range chart for the Wulalike Formation at well R16

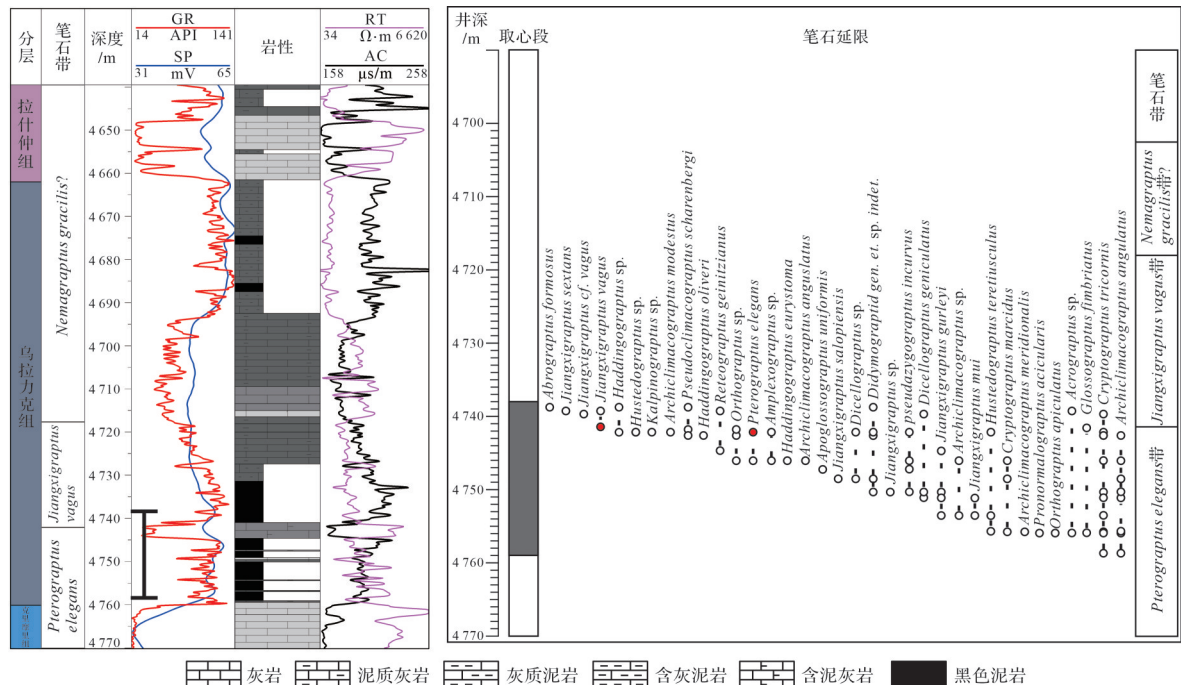


图 12 QT9 井乌拉力克组笔石延限图

Fig.12 Graptolite range chart for the Wulalike Formation at well QT9

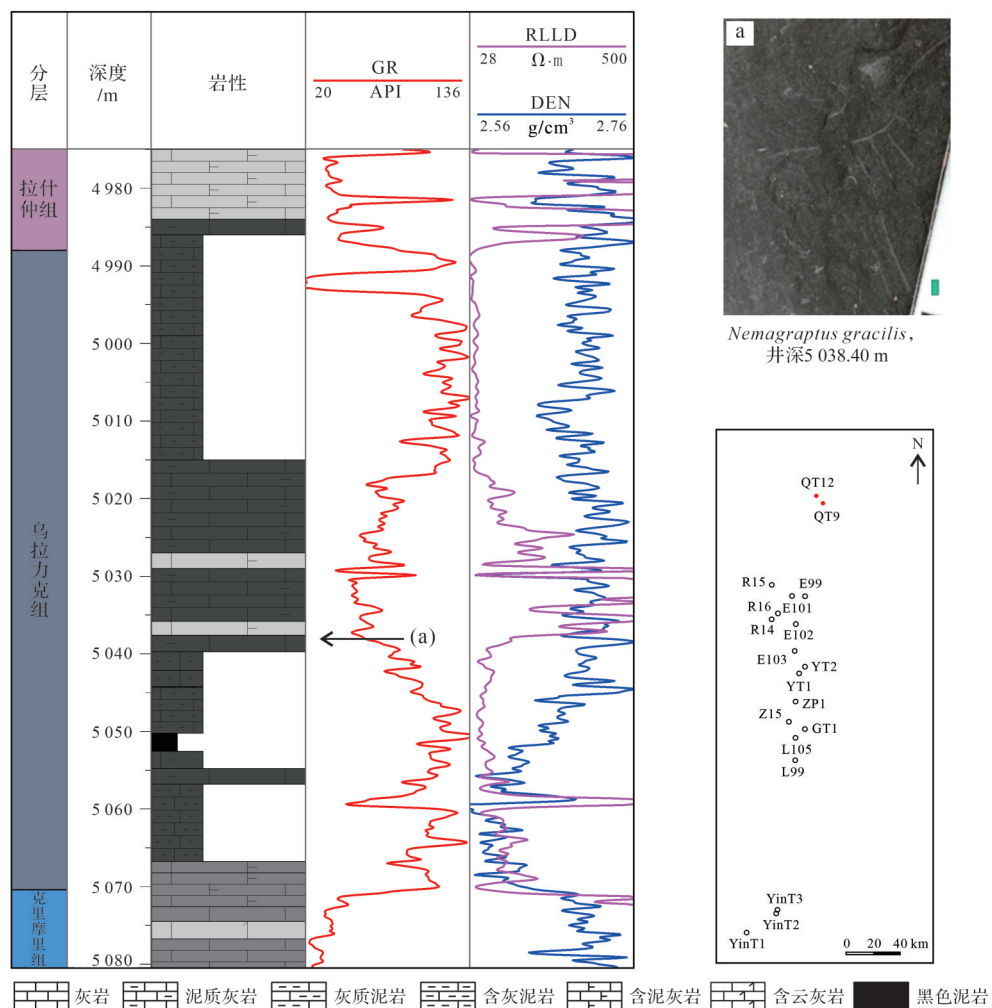


图 13 QT12 井乌拉力克组单井柱状图

Fig.13 Single well histogram of the Wulalike Formation at well QT12

(图 15)。由于 *Pseudazygograptus incurvus* 笔石化石在 3 959.00 m 以上出现, 据乌拉力克组底界 9.50 m, 暂将 *Nemagraptus gracilis* 带底界置于乌拉力克组底界。

3.2 生物地层格架建立

研究区位于鄂尔多斯盆地中央古隆起西部, 奥陶系时期受构造活动与海侵的影响, 致使研究区发育大量深灰色—黑色页岩、灰质泥岩、泥质灰岩及灰岩^[39-40], 沉积环境复杂, 导致对地层展布及发育特征认识不足。本文通过分析研究区 6 口钻井取心段的笔石带特征, 建立生物地层格架(图 16)。

受取心的限制, E102 井、E103 井与 YinT2 井的 *Nemagraptus gracilis* 带底界无法确定, 但经笔石鉴定认为, 这些井的取心段的底部整体表现为 *Nemagraptus gracilis* 带。由于取心段 *Nemagraptus gracilis* 及与其共生的笔石距乌拉力克组底界相对较近, 例如 YinT2 井, *Jiangxigraptus sextans* 笔化

石出现的位置距黑色页岩底界约 6.00 m, 故暂将这些井乌拉力克组的 *Nemagraptus gracilis* 带底界置于乌拉力克组底界(图 16), 由于样品缺失无法确定 *Nemagraptus gracilis* 带是否可以下延至克里摩里组。L105 井中与 *Nemagraptus gracilis* 笔石共生的笔化石 *Reteograptus geinitzianus* 距黑色页岩底界约 19.00 m, 但由于该井的黑色页岩厚度相对于 YinT2 井、E103 井较薄, 地势相对较高, 其乌拉力克组页岩的沉积时代相对于 E103 井与 YinT2 井较晚, 故将该井乌拉力克组的 *Nemagraptus gracilis* 带也暂定于乌拉力克组底界(图 16)。

通过笔石生物带划分发现, 乌拉力克组底部页岩从 QT9 井的 *Pterograptus elegans* 生物带到 R16 井的 *Jiangxigraptus vagus* 生物带和 E102 井、YinT2 井的 *Nemagraptus gracilis* 生物带是跨时的。QT9 井 *Pterograptus elegans* 的出现, 表明乌拉力克组页岩首

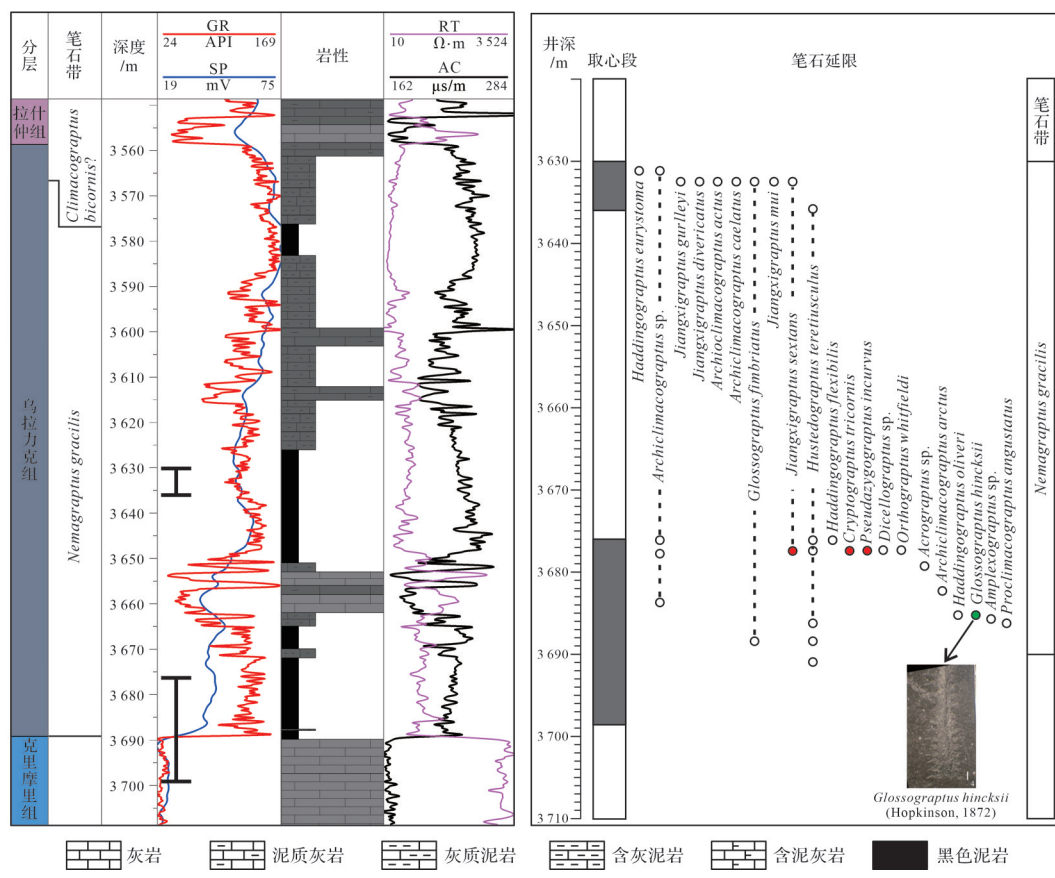


图 14 E102 井乌拉力克组笔石延限图

Fig.14 Graptolite range chart for the Wulalike Formation at well E102

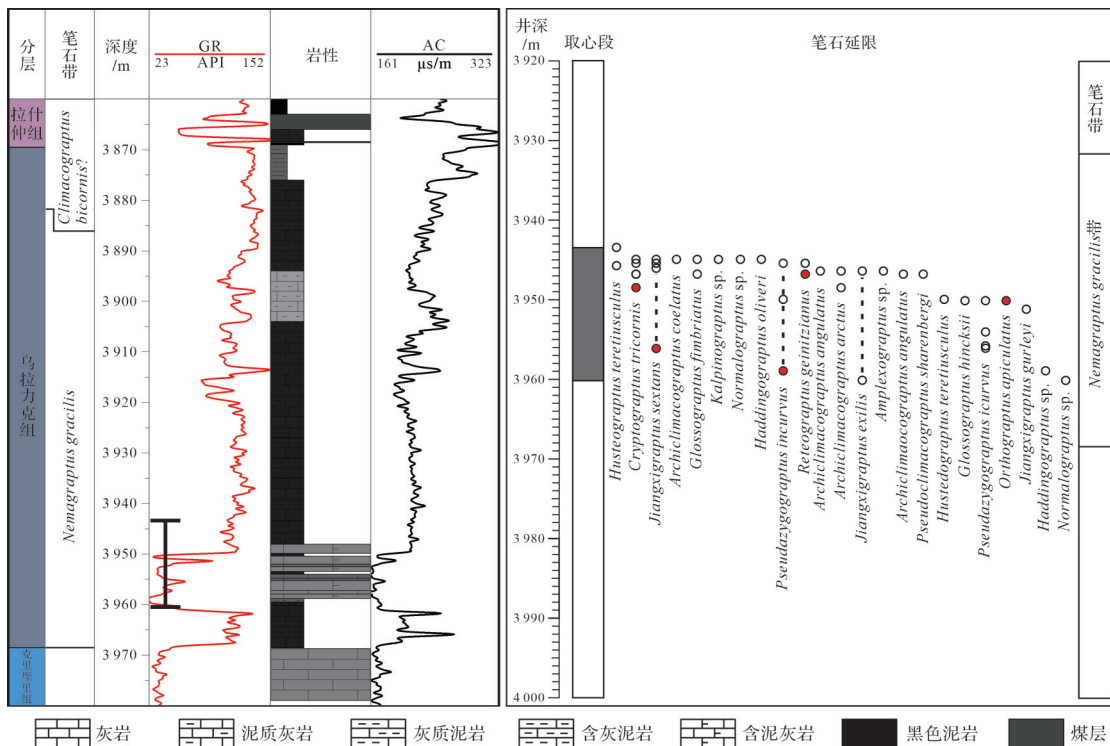


图 15 E103 井乌拉力克组笔石延限图

Fig.15 Graptolite range chart for the Wulalike Formation at well E103

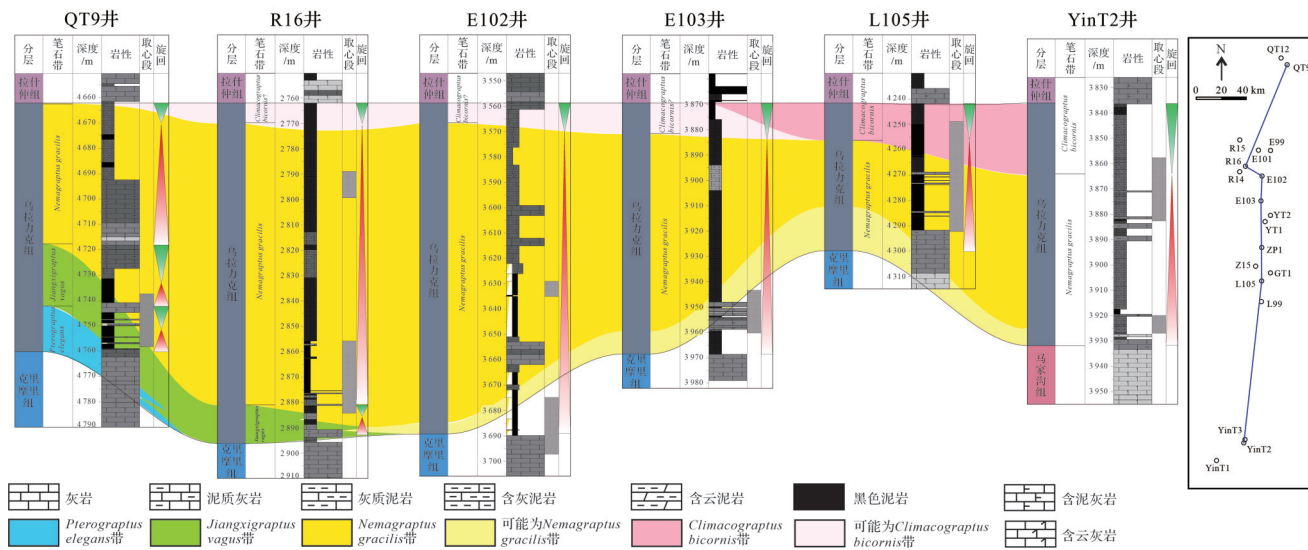


Fig.16 QT9井—YinT2井乌拉力克组笔石生物地层格架
Fig.16 Biostratigraphic framework for graptolites in the Wulalike Formation, wells QT 9 to YinT 2

先在QT9井一带沉积,至桑比早期,黑色页岩迁移至R16井一带以南进行沉积,沉积中心向南迁移,故乌拉力克组底部黑色页岩的分布具有强烈的穿时性,具有沿鄂尔多斯地块西缘向南变年轻的趋势。

陈旭等^[23]分析QT9井北部的内蒙古乌海大石门剖面的笔石化石,建立了克里摩里组—乌拉力克组的笔石分带(图17),但其对乌拉力克组的划分与本文所采用的划分方案有一定差异。目前,大多数学

者将克里摩里组大套灰岩以上的页岩作为乌拉力克组^[9,12,14,41-42],本文也采用该方案。对比认为大石门剖面的乌拉力克组同样发育*Pterograptus elegans*带,而乌拉力克组底部的页岩时代可能延伸至*Cryptograptus gracilicornis*层,故大石门剖面乌拉力克组底部页岩的形成时代可能更老,与本文所述的黑色页岩由北向南逐渐变年轻的观点吻合。张成弓^[43]对中央古隆起的构造演化分析认为,在中—晚奥陶世(乌拉力克组—拉什仲组),研究区整体呈现自东向西,自北向南,地层厚度逐渐增加,且秦祁海域范围逐渐缩小,沉积区向南逐渐萎缩,与本文沉积中心向南迁移的研究结果不谋而合。

4 讨论

4.1 黑色页岩的穿时性对沉积演化的探讨

对于黑色页岩的穿时性,存在两种可能。其一是在*Pterograptus elegans*带QT9井黑色页岩沉积时,南部可能为克里摩里组的碳酸盐岩台地相沉积;至桑比早期,R16井一带及其以南,成为沉积中心,也即因北部碳酸盐岩台地的向南扩增,黑色页岩向南迁移至本区;至桑比晚期,黑色页岩更向南迁移至L105井、YinT2井一带(图18)。这种发育模式表现为一个“降积准层序组叠置”的典型特征,即每个单元向海、向下迁移,各单元之间相变明显^[44],界面以下为深水相(黑色页岩沉积为主),界面以上为浅水相(以灰岩沉积为主),构成向上变浅的叠置样式(图18),黑色页岩穿

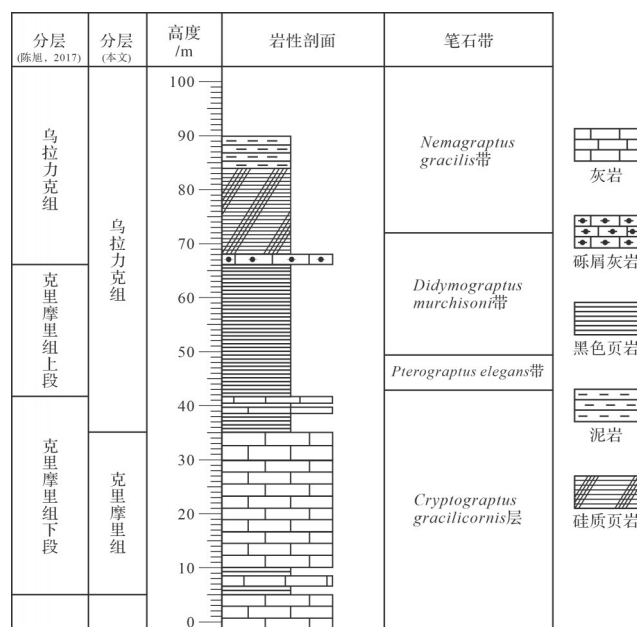


图 17 内蒙古乌海大石门剖面笔石分带图
(据文献[23]修改)

Fig.17 Graptolite zonation in the Dashimen Section in Wuhai, Inner Mongolia (modified from reference [23])

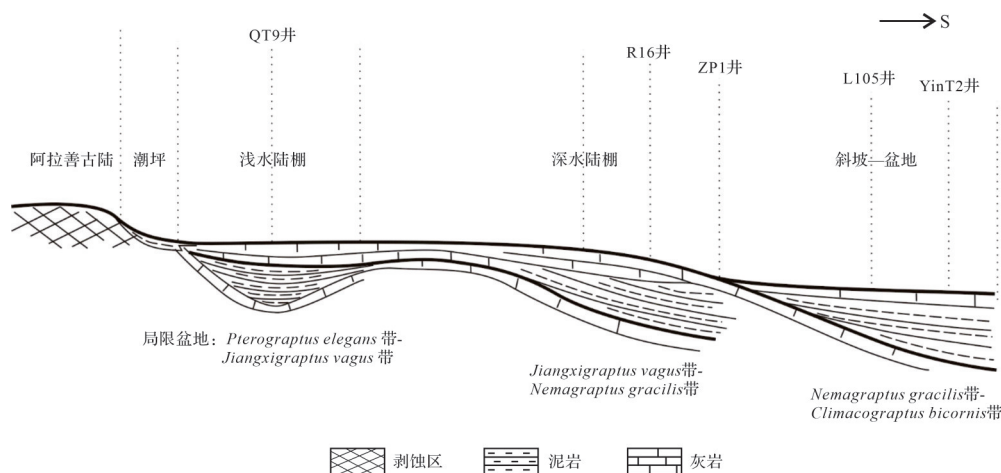


图 18 乌拉力克组黑色笔石页岩的演化模式
Fig.18 Evolution model of black graptolitic shale in the Wulalike Formation

过强制性海退界面。乌拉力克组内的一些砾屑灰岩层底面可能就是强制性海退界面。但是该模式需要确定工区南部乌拉力克组底部灰岩与 QT9 井乌拉力克组顶部灰岩的时代,由于取心的限制本文未获取相关的岩心样品,难以获取二者时代信息。

其二是乌拉力克组页岩的穿时性也可能是由海侵沉积以及在最大海泛面之后在高水位体系状态下的进积过程所造成,黑色页岩向南或向西南方向进积,北部水体向上逐渐变浅。这种模式依然缺乏南部乌拉力克组黑色页岩下方的灰岩时代来证明,并且还需确定研究区的物源方向。由于目前资料的限制,对于乌拉力克组黑色页岩穿时性的成因还需在之后的研究中收集更多的岩心样品,结合地震资料做进一步探讨。

由于工区北部 QT9 井—E103 井乌拉力克组顶部未取心,导致无法明确 *Climacograptus bicornis* 带是否在乌拉力克组顶部发育,但根据降积准层序组叠置的模式,工区北部乌拉力克组 *Climacograptus bicornis* 带可能逐渐缺失, *Nemagraptus gracilis* 带上延至拉什仲组。前人通过对内蒙古桌子山地区的笔石化石分析认为拉什仲组底部含 *Nemagraptus gracilis* 笔石化石,推断 *Nemagraptus gracilis* 带可延伸至拉什仲组,也可证明乌拉力克组的 *Climacograptus bicornis* 带由南向北可能逐渐缺失^[21]。

4.2 乌拉力克组海平面的相对变化

依据生物进化论理论,生物与其生存环境之间存在着相互影响、相互制约的密切关系。在沉积环境改变的同时,笔石生存环境也发生了改变,影响着

笔石的发育特征及笔石遗体的保存状态^[45],通过分析笔石的发育特征可反映沉积环境的变化^[5,46]。前人研究认为,在中奥陶世达瑞威尔阶—晚奥陶世桑比阶发生了非常引人注目的笔石特化事件,包括笔石体的复杂化、体壁退化、胞管褶皱等^[47],该时期的笔石特化事件可能形成于一个具有丰富营养物质的安静水体环境。上述特化事件与最大海泛面相吻合,暗示在最大海泛期,笔石生物为应对生存环境所发生的适应性变革,一是增加浮游能力,二是增强摄食能力,三是应对被捕食的生存竞争压力^[47-49]。这期间的特化事件,突出表现在 *Nemagraptus gracilis* 带和 *Pterograptus elegans* 带,换言之,这两个笔石带沉积期间,是鄂尔多斯盆地发生海侵的两个重要时期,但前者的范围局限,后者的分布范围明显广于前者。图 19 为工区内笔石复杂化的典型代表。*Nemagraptus gracilis*(图 19b)由两个纤细的单列笔石枝组成,每个主枝外侧着生若干辐射状排列的次枝,*Pterograptus elegans*(图 19c)下斜生长的主枝及从主枝上交互生长的侧枝组成,*Syndyograptus sinensis*(图 19a)由两个主枝和数对次枝(幼枝)组成。与普通的笔石相比,笔石枝明显增多,呈现复杂化。

基于岩性和复杂化笔石体的发育认为,研究区乌拉力克组存在两个海侵期。首先为乌拉力克组底部,其泥岩与下伏克里摩里组灰岩接触,说明水体加深,工区北部 QT9 井附近发育 *Pterograptus elegans* 带,而工区南部不发育,说明海侵从工区北部开始;*Jiangxigraptus vagus* 带同样在 QT9 井附近发育,岩性由泥岩、灰质泥岩过渡为灰岩,伽马曲线值降低,说明

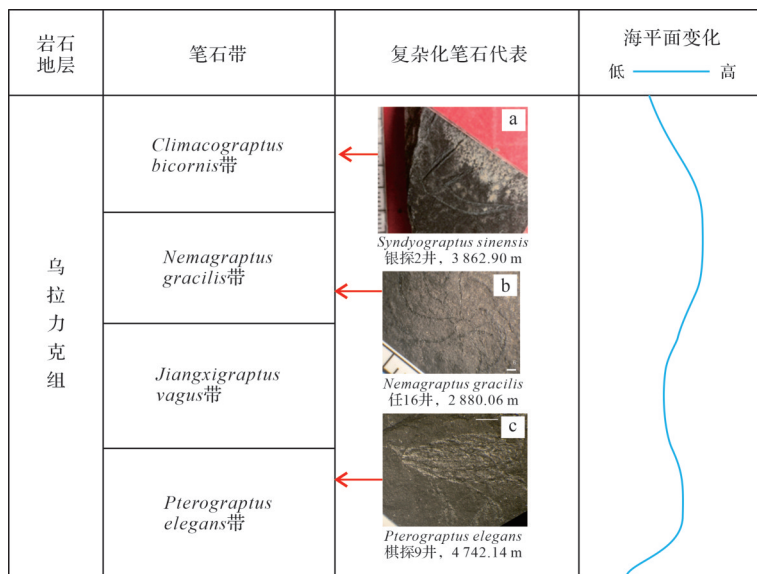


图 19 笔石形态的复杂化与相对海平面变化

Fig.19 Complexity of graptolite morphology relative to sea-level change

乌拉力克组 *Jiangxigraptus vagus* 带是一个海退期;而 *Nemagraptus gracilis* 带全区发生大范围海侵,岩性以泥岩与灰质泥岩为主,乌拉力克组开始大面积沉积;对于 *Climacograptus bicornis* 带,本次研究只在工区南部发现相应的笔石化石,其岩性由泥灰岩过渡为顶部拉什仲组的灰岩,说明该时期整体为一个海退期。

5 结论

(1) 研究区乌拉力克组笔石化石鉴定表明,其时代为奥陶世中晚期达瑞威尔阶—桑比阶,可划分为4个笔石带(自下而上:*Pterograptus elegans*、*Jiangxigraptus vagus*、*Nemagraptus gracilis*、*Climacograptus bicornis*)。研究区北部主要发育 *Pterograptus elegans* 与 *Jiangxigraptus vagus* 带,南部以 *Nemagraptus gracilis* 带为主。

(2) 笔石带划分揭示出乌拉力克组黑色页岩由鄂尔多斯盆地西缘北部向南逐渐变年轻,表明沉积中心逐渐向南迁移。乌拉力克组整体为海进—海退的过程,期间存在两次海侵期,发育于 *Pterograptus elegans* 与 *Nemagraptus gracilis* 带,前者海侵范围相对局限,主要发生在工区北部,后者海侵范围较广,促使乌拉力克组在盆地西缘大范围沉积。

致谢 感谢课题组全体人员的辛勤付出,感谢王传尚老师、何文祥老师、胡勇老师的耐心指导以及长庆油田勘探开发研究院的大力支持,使本文得以顺利完成。感谢两位评审专家提出的宝贵意见,使本文得以不断完善!

参考文献(References)

- [1] 付锁堂,付金华,席胜利,等.鄂尔多斯盆地奥陶系海相页岩气地质特征及勘探前景[J].中国石油勘探,2021,26(2):33-44.
[Fu Suotang, Fu Jinhua, Xi Shengli, et al. Geological characteristics of Ordovician marine shale gas in the Ordos Basin and its prospects[J]. China Petroleum Exploration, 2021, 26(2): 33-44.]
- [2] 刘子铭,付斯一,魏柳斌,等.鄂尔多斯盆地西缘中—晚奥陶世沉积演化特征及古环境分析[J].矿物岩石,2024,44(2):177-193. [Liu Ziming, Fu Siyi, Wei Liubin, et al. Sedimentary evolution characteristics and paleoenvironmental analysis of the Ordovician in the western margin of the Ordos Basin[J]. Mineralogy and Petrology, 2024, 44(2): 177-193.]
- [3] 张元动,陈旭.奥陶纪笔石动物的多样性演变与环境背景[J].中国科学:地球科学,2008,38(1):10-21. [Zhang Yuandong, Chen Xu. Diversity history of Ordovician graptolites and its relationship with environmental change[J]. Science China Earth Sciences, 2008, 38(1): 10-21.]
- [4] 邹才能,龚剑明,王红岩,等.笔石生物演化与地层年代标定在页岩气勘探开发中的重大意义[J].中国石油勘探,2019,24(1):1-6. [Zou Caineng, Gong Jianming, Wang Hongyan, et al. Importance of graptolite evolution and biostratigraphic calibration on shale gas exploration[J]. China Petroleum Exploration, 2019, 24 (1): 1-6.]
- [5] 张娣,刘伟,周业鑫,等.扬子区西南缘奥陶纪末—志留纪初笔石生物地层对比及意义[J].沉积与特提斯地质,2022,42(3):413-425. [Zhang Di, Liu Wei, Zhou Yexin, et al. Biostratigraphic correlation of graptolites from Late Ordovician to Early Silurian on the southwestern margin of the Yangtze region[J]. Sedimentary Geology and Tethyan Geology, 2022, 42(3): 413-425.]
- [6] 梁峰,王红岩,拜文华,等.川南地区五峰组—龙马溪组页岩笔

- 石带对比及沉积特征[J]. 天然气工业, 2017, 37(7):20-26. [Li-ang Feng, Wang Hongyan, Bai Wenhua, et al. Graptolite correlation and sedimentary characteristics of Wufeng-Longmaxi shale in southern Sichuan Basin[J]. Natural Gas Industry, 2017, 37(7): 20-26.]
- [7] 白灵麒,金小赤,刘建波,等. 内蒙古苏尼特左旗北部中—上奥陶统巴彦呼舒组地层划分与沉积环境分析[J]. 地层学杂志, 2019, 43(4) : 442-452. [Bai Lingqi, Jin Xiaochi, Liu Jianbo, et al. Stratigraphic subdivision and depositional environment of the Middle-Upper Ordovician Bayanhushu Formation in northern spongid Zuoqi of Inner Mongolia[J]. Journal of Stratigraphy, 2019, 43(4): 442-452.]
- [8] 傅力浦,胡云绪,张子福,等. 鄂尔多斯中、上奥陶统沉积环境的生物标志[J]. 西北地质科学, 1993, 14(2):1-96. [Fu Lipu, Hu Yunxu, Zhang Zifu, et al. The mark on the ecology of Sedimentary environment in Middle and Upper Ordovician at Ordos Basin [J]. Northwest Geoscience, 1993, 14(2): 1-96.]
- [9] 马占荣,白海峰,刘宝宪,等. 鄂尔多斯西部地区中—晚奥陶世克里摩里期—乌拉力克期岩相古地理[J]. 古地理学报, 2013, 15(6) : 751-764. [Ma Zhanrong, Bai Haifeng, Liu Baoxian, et al. Lithofacies palaeogeography of the Middle-Late Ordovician Keli-moli and Wulalike Ages in western Ordos area[J]. Journal of Palaeogeography, 2013, 15(6): 751-764.]
- [10] 张文华,徐怀大,王广昀,等. 桌子山奥陶系沉积层序特征[M]. 北京:石油工业出版社, 1996; 1-83. [Zhang Wenhua, Xu Huaida, Wang Guangyun, et al. Characteristics of the Ordovician sedimentary sequence in Zhuozi Mountain[M]. Beijing: Petroleum Industry Press, 1996: 1-83.]
- [11] 孙肇才,胡显穆. 鄂尔多斯盆地西南缘奥陶系的对比划分意见及其对中西部油气勘探的意义[J]. 海相油气地质, 2002, 7(4) : 41-58. [Sun Zhaocai, Hu Xianmu. View on the correlation and demarcation of the Ordovician series in the southwestern margin region of Ordos Basin and the significance of petroleum exploration in central-western part of China[J]. Marine Origin Petroleum Geology, 2002, 7(4): 41-58.]
- [12] 于洲,周进高,李程善,等. 鄂尔多斯盆地西缘奥陶纪克里摩里期—乌拉力克期构造—岩相古地理特征[J]. 天然气地球科学, 2021, 32(6) : 816-825. [Yu Zhou, Zhou Jingao, Li Cheng-shan, et al. Tectonic-lithofacies paleogeographic characteristics of Ordovician Kelimoli and Wulalike stages in the western edge of Ordos Basin[J]. Natural Gas Geoscience, 2021, 32(6): 816-825.]
- [13] 孙华丽,高建荣,付玲,等. 鄂尔多斯盆地西缘奥陶系古环境恢复及沉积体系分析[J]. 东北石油大学学报, 2023, 47(1):44-56, 69. [Sun Huali, Gao Jianrong, Fu Ling, et al. Restoration of Ordovician paleoenvironment and analysis of sedimentary system in the western margin of Ordos Basin[J]. Journal of North-east Petroleum University, 2023, 47(1): 44-56, 69.]
- [14] 席胜利,莫午零,刘新社,等. 鄂尔多斯盆地西缘奥陶系乌拉力克组页岩气勘探潜力:以忠平1井为例[J]. 天然气地球科学, 2021, 32(8) : 1235-1246. [Xi Shengli, Mo Wuling, Liu Xinshe, et al. Shale gas exploration potential of Ordovician Wulalike Formation in the western margin of Ordos Basin: Case study of well Zhongping 1[J]. Natural Gas Geoscience, 2021, 32(8): 1235-1246.]
- [15] 冯弋秦. 鄂尔多斯盆地西北缘乌拉力克组泥页岩储层特征及成藏模式研究[D]. 成都:成都理工大学, 2020: 1-74. [Feng Yiqin. Reservoir characteristics and accumulation model of mud shale of Wulalik Formation in northwestern margin of Ordos Basin[D]. Chengdu: Chengdu University of Technology, 2020: 1-74.]
- [16] 吴东旭,吴兴宁,李程善,等. 鄂尔多斯盆地西部奥陶系乌拉力克组烃源岩沉积模式及生烃潜力[J]. 海相油气地质, 2021, 26(2) : 123-130. [Wu Dongxu, Wu Xingning, Li Chengshan, et al. Sedimentary model and hydrocarbon-generation potential of source rock of the Ordovician Ulalik Formation in western Ordos Basin[J]. Marine Origin Petroleum Geology, 2021, 26(2): 123-130.]
- [17] 席胜利,郑聪斌,李振宏. 鄂尔多斯盆地西缘奥陶系地球化学特征及其沉积环境意义[J]. 古地理学报, 2004, 6(2):196-206. [Xi Shengli, Zheng Congbin, Li Zhenhong. Geochemical characteristics and its sedimentary environment significance of the Ordovician in western margin of Ordos Basin[J]. Journal of Palaeogeography, 2004, 6(2): 196-206.]
- [18] 朱淑玥,刘磊,王峰,等. 鄂尔多斯盆地西缘及邻区石炭系羊虎沟组砂体成因机制与沉积过程[J]. 沉积学报, 2023, 41(4): 1153-1169. [Zhu Shuyue, Liu Lei, Wang Feng, et al. Genetic mechanism and depositional processes of sandy sediments from the Carboniferous Yanghugou Formation along the western margin of the Ordos Basin and its adjacent areas[J]. Acta Sedimentologica Sinica, 2023, 41(4): 1153-1169.]
- [19] 赵裕亭. 浙江江山衢县一带宁国组中的对笔石[C]//中国地质科学院地层古生物论文集编委会. 地层古生物论文集(第三辑). 北京:地质出版社, 1977: 86-107. [Zhao Yuting. The Didymograptus species in the Ningguo Formation in the area of Jiangshan and Quxian, Zhejiang[C]//Editorial Committee of the Collection of Papers on Stratigraphic Paleontology, Chinese Academy of Geological Sciences. Collection of Papers on Stratigraphic Paleontology (Volume 3). Beijing: Geological Publishing House, 1977: 86-107.]
- [20] 张元动,詹仁斌,甄勇毅,等. 中国奥陶纪综合地层和时间框架[J]. 中国科学:地球科学, 2019, 49(1):66-92. [Zhang Yuandong, Zhan Renbin, Zhen Yongyi, et al. Ordovician integrative stratigraphy and timescale of China[J]. Science China Earth Sciences, 2019, 49(1): 66-92.]
- [21] 张元动,詹仁斌,王志浩,等. 中国奥陶纪地层及标志化石图集[M]. 杭州:浙江大学出版社, 2020: 1-575. [Zhang Yuandong, Zhan Renbin, Wang Zhihao, et al. Ordovician stratigraphy and index fossils of China[M]. Hangzhou: Zhejiang University Press, 2020: 1-575.]

- [22] Maletz J, Ahlberg P, Lundberg F. Ordovician graptolite biostratigraphy of the Röstånga-2 drill core (Scania, southern Sweden) [J]. GFF, 2020, 142(3): 206-222.
- [23] 陈旭, 张元动, 丹尼尔·古特曼, 等. 中国西北地区奥陶系达瑞威尔阶至凯迪阶的笔石研究[M]. 杭州: 浙江大学出版社, 2017: 1-321. [Chen Xu, Zhang Yuandong, Goldman D, et al. Darriwilian to Katian (Ordovician) graptolites from northwest China[M]. Hangzhou: Zhejiang University Press, 2017: 1-321.]
- [24] 王志浩, 伯格斯特龙, 甄勇毅, 等. 内蒙古乌海大石门奥陶系牙形刺和Histiodella动物群发现的意义[J]. 微体古生物学报, 2013, 30(4): 323-343. [Wang Zhihao, Bergström S, Zhen Yongyi, et al. Ordovician Conodonts from Dashimen, Wuhai in inner Mongolia and the significance of the discovery of the Histiodella fauna[J]. Acta Micropalaeontologica Sinica, 2013, 30(4): 323-343.]
- [25] Bergström S M, Wang Z H, Goldman D. Relations between Darriwilian and Sandbian conodont and graptolite biozones[M]// Chen X, Bergström S M, Finney S C, et al. Darriwilian to Katian (Ordovician) graptolites from northwest China. Amsterdam: Elsevier, 2015: 39-78.
- [26] Goldman D, Nölvak J, Maletz J. Middle to Late Ordovician graptolite and chitinozoan biostratigraphy of the Kandava-25 drill core in western Latvia[J]. GFF, 2015, 137(3): 197-211.
- [27] Maletz J, Egenhoff S, Böhme M, et al. The Elnes Formation of southern Norway: Key to the Middle Ordovician biostratigraphy & biogeography[J]. Acta Palaeontologica Sinica, 2007, 46(Suppl.): 298-304.
- [28] Chen X, Zhang Y D, Daniel G, et al. Darriwilian to Katian (Ordovician) Graptolites from northwest China[M]. Hangzhou: Zhejiang University Press, 2016: 1-370.
- [29] Finney S C, Bergstrom S M, Chen X, et al. The Pingliang section, Gansu province, China: Potential as global stratotype for the base of the Nemagraptus gracilis Biozone and the base of the global Upper Ordovician Series[J]. Acta Universitatis Carolinae-Geologica, 1999, 43(1/2): 73-76.
- [30] Bergström S M, Finney S C, Xu C, et al. A proposed global boundary stratotype for the base of the Upper series of the Ordovician system: The Fågelsång section, Scania, southern Sweden [J]. Episodes, 2000, 23(2): 102-109.
- [31] 樊茹, 马雪莹, 吕丹, 等. 甘肃平凉上奥陶统牙形石和笔石生物地层[J]. 地质学报, 2020, 94(11): 3213-3227. [Fan Ru, Ma Xueying, Lü Dan, et al. Upper Ordovician conodont and graptolite biostratigraphy of Pingliang, Gansu province, China[J]. Acta Geologica Sinica, 2020, 94(11): 3213-3227.]
- [32] 董轶婷, 刘建波, 陈宇轩, 等. 早—中奥陶世华南古海洋氧化还原变化及其对奥陶纪生物大辐射的意义[J]. 北京大学学报(自然科学版), 2018, 54(4): 739-751. [Dong Yiting, Liu Jianbo, Chen Yuxuan, et al. Redox variation during the early and Middle Ordovician in South China and its implication to the great Ordovician Biodiversification event[J]. Acta Scientiarum Naturalium Universitatis Pekinensis, 2018, 54(4): 739-751.]
- [33] 陈旭, 张元动, 李越, 等. 塔里木盆地及周缘奥陶系黑色岩系的生物地层学对比[J]. 中国科学: 地球科学, 2012, 42(8): 1173-1181. [Chen Xu, Zhang Yuandong, Li Yue, et al. Biostratigraphic correlation of the Ordovician black shales in Tarim Basin and its peripheral regions[J]. Science China Earth Sciences, 2012, 42(8): 1173-1181.]
- [34] 付力浦. 陕西陇县龙门洞中奥陶世笔石分带[J]. 西北地质, 1979(4): 23-37. [Fu Lipu. Middle ordovian graptolite zone of Longxian, and discription of some Midde Ordovician climaograptus[J]. Northwestern Geology, 1979(4): 23-37.]
- [35] Chen X, Bergström S M, Zhang Y D, et al. Upper Ordovician (Sandbian-Katian) graptolite and conodont zonation in the Yangtze region, China[J]. Earth and Environmental Science Transactions of the Royal Society of Edinburgh, 2010, 101(2): 111-134.
- [36] 俞剑华, 方一亭, 刘怀宝. 安徽省宁国县胡乐地区含笔石地层研究新进展[J]. 中国地质科学院院报, 1986(1): 25-34. [Yu Jianhua, Fang Yiting, Liu Huabao. New advances in the Ordovician graptolite-bearing strata from the Hule area in Ningguo county, southern Anhui[J]. Acta Geoscientica Sinica, 1986(1): 25-34.]
- [37] Cooper R A, Maletz J, Taylor L, et al. Graptolites: Patterns of diversity across paleolatitudes[M]//Webby B D, Paris F, Droser M L, et al. The great Ordovician biodiversification event. New York: Columbia University Press, 2004: 281-293.
- [38] 张元动, 陈旭, Goldman D, 等. 华南早—中奥陶世主要环境下笔石动物的多样性与生物地理分布[J]. 中国科学: 地球科学, 2010, 40(9): 1164-1180. [Zhang Yuandong, Chen Xu, Goldman D, et al. Diversity and paleobiogeographic distribution patterns of Early and Middle Ordovician graptolites in distinct depositional environments of South China[J]. Science China Earth Sciences, 2010, 40(9): 1164-1180.]
- [39] 邓昆, 张哨楠, 周立发, 等. 鄂尔多斯盆地古生代中央古隆起形成演化与油气勘探[J]. 大地构造与成矿学, 2011, 35(2): 190-197. [Deng Kun, Zhang Shaonan, Zhou Lifá, et al. Formation and tectonic evolution of the Paleozoic central Paleouplift of Ordos Basin and its implications for oil-gas exploration[J]. Geotectonica et Metallogenica, 2011, 35(2): 190-197.]
- [40] 邵东波, 包洪平, 魏柳斌, 等. 鄂尔多斯地区奥陶纪构造古地理演化与沉积充填特征[J]. 古地理学报, 2019, 21(4): 537-556. [Shao Dongbo, Bao Hongping, Wei Liubin, et al. Tectonic palaeogeography evolution and sedimentary filling characteristics of the Ordovician in the Ordos area[J]. Journal of Palaeogeography, 2019, 21(4): 537-556.]
- [41] 李福奇, 王晓锋, 刘文汇, 等. 鄂尔多斯盆地西缘奥陶系乌拉力克组页岩气地球化学特征与成因[J]. 天然气地球科学, 2025, 35(9): 1626-1637. [Li Fuqi, Wang Xiaofeng, Liu Wenhui, et al. Geochemical characteristics and genesis of shale gas in the Ordovician Wulalik Formation in the western, Ordos Basin[J]. Natural Gas Geoscience, 2025, 35(9): 1626-1637.]

- [42] 于洲, 黄正良, 李维岭, 等. 鄂尔多斯盆地中奥陶统乌拉力克组海相页岩岩相类型及优质储层发育特征[J]. 天然气工业, 2023, 43(3): 23-33. [Yu Zhou, Huang Zhengliang, Li Weiling, et al. Lithofacies types and high-quality reservoir development characteristics of marine shale in the Middle Ordovician Wulalike Formation, Ordos Basin[J]. Natural Gas Industry, 2023, 43(3): 23-33.]
- [43] 张成弓. 鄂尔多斯盆地早古生代中央古隆起形成演化与物质聚集分布规律[D]. 成都: 成都理工大学, 2013: 1-114. [Zhang Chenggong. Forming evolution and sediments accumulation & distribution regularity of central paleouplift in Eopaleozoic, Ordos Basin[D]. Chengdu: Chengdu University of Technology, 2013: 1-114.]
- [44] Lin W, Bhattacharya J P, Stockford A. High-resolution sequence stratigraphy and implications for Cretaceous glacioeustasy of the Late Cretaceous Gallup system, New Mexico, U. S. A. [J]. Journal of Sedimentary Research, 2019, 89(6): 552-575.
- [45] 易定鑫, 田景春, 井翠, 等. 五峰组—龙马溪组笔石带划分与沉积环境的意义:以重庆武隆接龙剖面为例[J]. 东北石油大学学报, 2019, 43(6): 33-43. [Yi Dingxin, Tian Jingchun, Jing Cui, et al. Graptolite biostratigraphy and sedimentary environment significance: A case study from the Wufeng Formation-Longmaxi Formation of Jielong Section in Wulong, Southeastern Chongqing[J]. Journal of Northeast Petroleum University, 2019, 43(6): 33-43.]
- [46] 李刚, 赵迪斐, 郭英海. 川东南地区龙马溪组页岩笔石与沉积环境的关系[J]. 科学技术与工程, 2018, 18(12): 16-23. [Li Gang, Zhao Difei, Guo Yinghai. The relationship between graptolite of Longmaxi shale and sedimentary environment in southeastern Sichuan[J]. Science Technology and Engineering, 2018, 18(12): 16-23.]
- [47] Ma X, Zhang Y D. On the morphological complexity of the graptolite Tubaria in the Darriwilian (Middle Ordovician)[J]. Acta Geologica Sinica-English Edition, 2019, 93(Supp. 3): 135-137.
- [48] 王传尚, 汪啸风, 陈孝红. 奥陶纪笔石体的复杂化及其与海平面变化的关系[J]. 华南地质与矿产, 2000, 16(1): 11-15. [Wang Chuanshang, Wang Xiaofeng, Chen Xiaohong. Relationships between Rhabdosome complication and Ordovician sea level changes[J]. Geology and Mineral Resources of South China, 2000, 16(1): 11-15.]
- [49] 王传尚, 汪啸风. 早—中奥陶世之交笔石动物群全球分布及其控制作用[J]. 地质科技情报, 2011, 30(2): 41-44, 51. [Wang Chuanshang, Wang Xiaofeng. Global distribution of graptolite fauna and its controlling factor during the Lower-Middle Ordovician transitional Period[J]. Geological Science and Technology Information, 2011, 30(2): 41-44, 51.]

Division of Graptolite Zones in the Wulalike Formation at the Western Margin of the Ordos Basin: Implications for sedimentary evolution

GAO XiaoYang¹, WANG ChuanShang², HE WenXiang¹, ZHANG JianWu³, FENG Li⁴, YAN JingWen¹, WAN Tao⁵, ZHU JianBin⁶, XU PengCheng³, WANG Bin⁷, HU Yong¹

1. College of Resources and Environmental Sciences, Yangtze University, Wuhan 430100, China

2. Hubei Key Laboratory of Paleontology and Geological Environment Evolution, Wuhan Center of China Geological Survey, Wuhan 430100, China

3. Research Institute of Exploration and Development, PetroChina Changqing Oilfield Company, Xi'an 710000, China

4. Exploration Division of PetroChina Changqing Oilfield Company, Xi'an 710018, China

5. Geophysical Research Institute, Zhongyuan Oilfield, SINOPEC, Puyang, Henan 457000, China

6. 1st Oil Plant of Changqing Oil Field, PetroChina, Yan'an, Shaanxi 716000, China

7. Changqing Industry Group Co. LTD, Petrochina Changqing Oilfield Company, Xi'an 710018, China

Abstract: [Objective] A set of black marine graptolitic shales is developed in the Wulalike Formation at the western margin of the Ordos Basin. In recent years, natural gas has continually been discovered in this set of shales and an industrial level of oil flow has been produced, demonstrating that the Wulalike Formation has significant exploration potential. This study examines the development of the graptolites and establishes a biostratigraphic framework as a basis for analyzing the sedimentary evolution of the Wulalike Formation. [Methods] The age range of the Wulalike Formation was clarified by analyzing the graptolite content of individual cored wells and comparing the graptolite range. Single-well graptolite zones were identified and biostratigraphic frameworks were constructed on that basis,

and the distribution of the graptolite zones is discussed. The spatial evolution of the black shale was analyzed in combination with the lithological development. Sea-level variation was also considered based on the response of graptolite morphological complexity to marine transgression. [Results] (1) The Wulalike Formation was developed during the Darriwilian-Sandbian stages at the end of the middle- and beginning of the Upper Ordovician. The Wulalike Formation is divided into four graptolite zones from bottom to top: the *Pterograptus elegans* zone, *Jiangxigraptus vagus* zone, *Nemagraptus gracilis* zone and *Climacograptus bicornis* zone. (2) From a comparative analysis of their development, it is believed that all four graptolite zones are developed in the northern Wulalike Formation of the study area in the vicinity of well QT9, while the *Pterograptus elegans* and *Jiangxigraptus vagus* zones are absent in the southern part of the Formation. (3) Two marine transgression periods are indicated by the *Pterograptus elegans* and *Nemagraptus gracilis* zones in the Wulalike Formation, transitioning upward into the *Climacograptus bicornis* zone and then into the Lashizhong Formation, during which time the sea level gradually lowered. [Conclusions] The black graptolitic shale at the bottom of the Wulalike Formation shows strong diachronism from *Pterograptus elegans* in well QT9 to *Nemagraptus gracilis* in well YinT2. Along the western margin of the Ordos Block, the strata are gradually younger to the south, and the deposition center gradually migrates southward. The diachronism is typically manifested as “degradational stacking”, evident as an upward-shallowing stacking pattern that indicates a forced marine regression interface. Alternatively, the diachronism of the black shale may be due to marine transgression deposition and progradation in a highstand systems tract, resulting in the progradation of the black shale towards the south or southwest. Due to the limitations of core sampling, in subsequent studies the causes of the diachronism of the black shale will require determination of the formation ages of the limestone at the top and bottom of the Wulalike Formation, along with verification by seismic data. The establishment of a biostratigraphic framework in this study based on the graptolite zonation provides important guidance for understanding the stratigraphic and sedimentary evolution of the Wulalike Formation at the western margin of the Ordos Basin.

Key words: graptolite zone division; biostratigraphic framework; Wulalike Formation; sedimentary evolution